BIPOLAR MOLECULAR OUTFLOWS

R. BACHILLER & M. TAFALLA
IGN Observatorio Astronómico Nacional
Apartado 1143, E-28800 Alcalá de Henares, Spain

1. Introduction

Stars form by the gravitational collapse of dense gas in molecular clouds, so one would naively expect that infall motions dominate the gas kinematics in star-forming regions. Observations, however, show this not to be the case, and that outflow motions —not infall— is what prevails around young stellar objects (YSOs). This apparent contradiction was fully realized about 20 years ago, when the first systematic molecular observations of star-forming regions were done, and bipolar molecular outflows were found towards almost every region of star formation (e.g, Snell et al. 1980, Bally & Lada 1983). The discovery of outflows has deeply changed our picture of how stars are born; their observational study has dominated the field of star formation research, and their theoretical understanding has posed a serious challenge to theorists of stellar birth. After 20 years of intense outflow research, enormous progress has been done, but some basic questions still remain unanswered. In this review we attempt to briefly describe what we know about molecular outflows, and also show the challenges that lie ahead in this exciting field of star formation.

Outflows driven by young stars and protostars are observable over a wide range of wavelengths, from the ultraviolet to the radio, so it is natural that the history of outflow research started with observations in the visible, the earliest developed astronomy tool. In the early 1950's, Herbig (1951) and Haro (1952) observed a few peculiar small nebulosities with emission line spectra. These so-called Herbig-Haro (HH) objects were soon associated with stellar winds (Osterbrok 1958), and later recognized to result from the interaction of highly supersonic stellar winds with ambient material (Schwartz 1975). Measurements of proper motions (Cudworth & Herbig 1979) and the detection of highly-collimated HH jets (Mundt & Fried 1983) confirmed that the wind ejection takes place in the vicinity of a newly formed star.

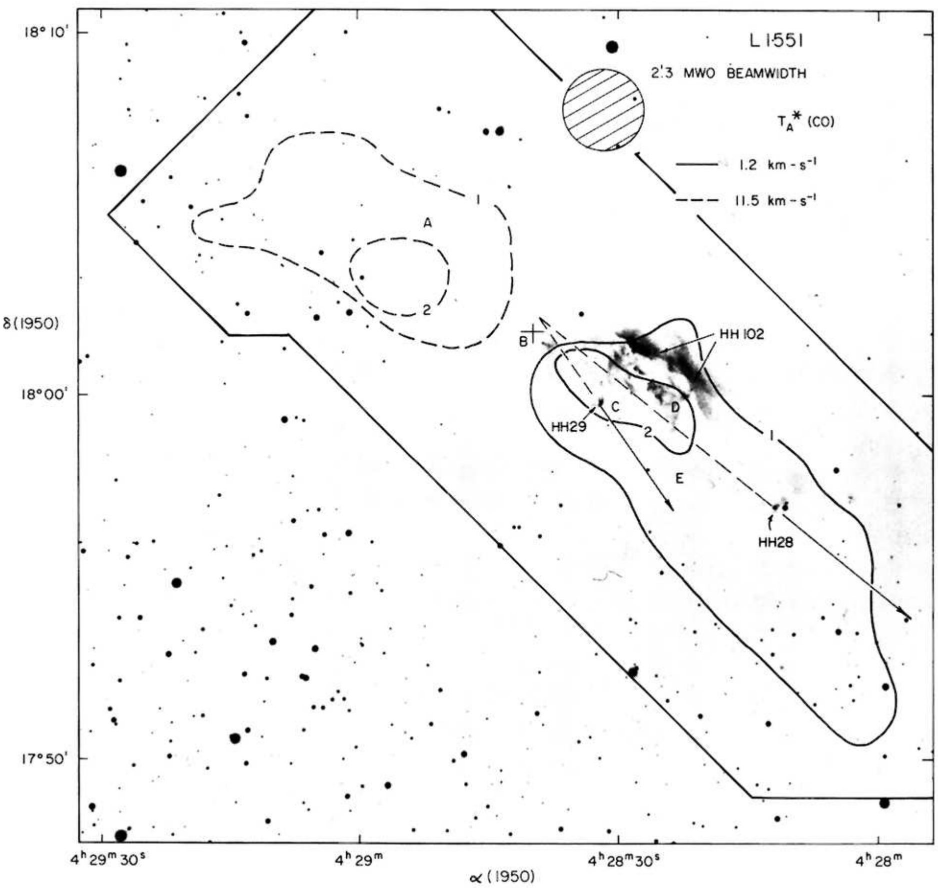

Figure 1. Contour map of the J=1–0 CO emission from the L1551 outflow superposed on an optical photograph of the region (from Snell et al. 1980). Solid contours represent blue shifted emission and dashed contours are red shifted emission. The cross indicates the position of the driving infrared source, IRS5. Also shown are the Herbig-Haro objects in the field. The directions of the proper motions of the two compact HH objects HH28 and HH29, which are also indicated, suggest a common origin at the infrared source

The presence of winds emerging from young stars was also suggested by the profile shapes of optical spectral lines (Herbig 1960; Kuhi 1964), the presence of centimeter wavelength free-free continuum emission (Cohen et al. 1982; Rodríguez 1995), and the detection of H_2 lines in the near infrared (Beckwith et al. 1978; Hodapp & Ladd 1995). When these winds interact with the surrounding molecular cloud, they give rise to molecular outflows, which are best observed in the millimeter-wave lines of carbon monoxide (CO). The first broad CO lines, indicative of high-velocity molecular gas, were discovered toward the Orion A molecular cloud in the mid 70's (Zuckerman

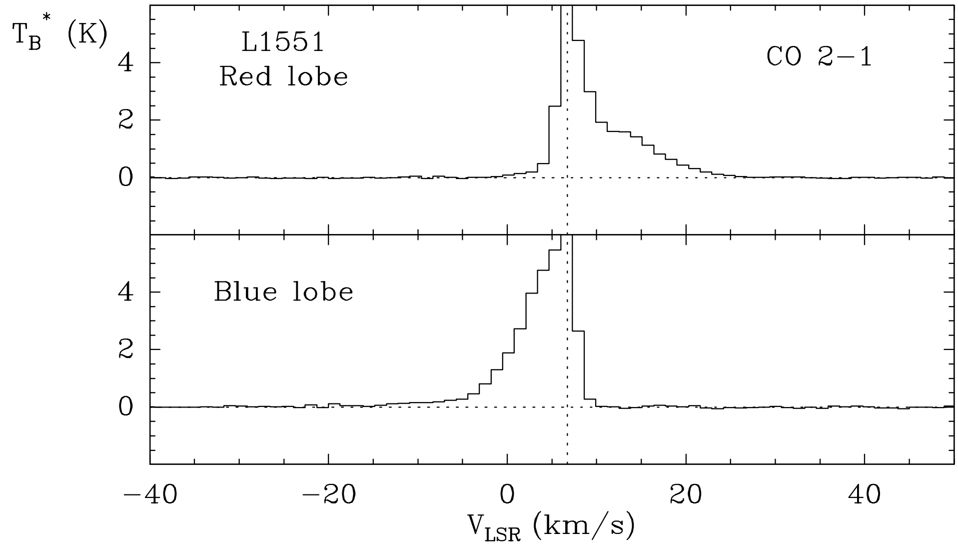

Figure 2. CO J=2–1 spectra averaged along the main axis of the L1551 outflow. The data (from Bachiller et al. 1994) were taken with the IRAM 30-m radio telescope, whose beam size is $\sim 12''$ at 230 GHz.

et al. 1976, Kwan & Scoville 1976), and soon thereafter detailed mapping of the supersonic CO emission in different objects showed that outflowing material tends to lie in two lobes of gas, one blue shifted and the other red shifted (Snell et al. 1980; Rodríguez et al. 1980; see Figs. 1 and 2). The field of bipolar outflow research was in this way born.

The first systematic outflow searches showed that these systems are extraordinarily common around young stars, and that stars of different masses have detectable flows (Bally & Lada 1983; Edwards & Snell 1982, 1983, 1984). The number of known outflows has increased rapidly over the last 20 years. Lada (1985) compiled a first catalog containing 68 outflow sources, Fukui et al. (1993) listed 157 outflows confirmed through complete or partial mapping, and Wu et al. (1997) have cataloged around 200 outflows. It is now believed that every star, no matter its mass, goes through an outflow phase during its early life, and that the outflow phenomenon is deeply connected to the process of star formation (e.g, Shu et al. 1987).

Since the review by Bally & Lane (1991) at the Crete I Advanced Study Institute, the study of bipolar outflows has benefited enormously from the use of the new generation of millimeter and submillimeter radio telescopes and interferometers. These new observations have revealed a population of highly collimated molecular outflows with extremely high velocity and evidence for strong interaction with the surrounding gas, which seems to correspond to the early phases of the outflow life. In this chapter, we review the basic properties of the more "classical" outflows (those identified during the 80's) and those of the highly collimated flows identified in the 90's, proposing an evolutionary sequence to connect them. We refer the reader to the chapter by Shu for the theoretical modeling of the outflow phenomenon, the chapter by Churchwell for more emphasis on outflows from high mass stars, and the chapter by Reipurth & Raga for a review of HH objects and jets. Other relevant recent reviews on molecular outflows include those by Bachiller (1996), Padman et al. (1997), Cabrit et al. (1997) and Richer et al. (1999). An up to date view of the current situation in outflow research is provided by a reading of the proceedings of the recent IAU Symposium 182.

2. Determining Outflow Properties from CO Observations

Molecular outflow gas is best traced by its CO emission, as this molecule is abundant, has a very simple level structure (it is a linear rotor), and different isotopes are detectable at millimeter wavelengths (^{12}CO, ^{13}CO, C^{18}O). Deriving outflow properties therefore requires converting CO line observations into physical gas parameters, and this makes CO radiative transfer the most useful tool of a molecular outflow observer. As the CO emission traces ambient gas swept up by the outflow over its lifetime (see below), CO observations provide a time integrated picture of the outflow activity. It is therefore a challenge for the astronomer to read the outflow history from the observed CO lines, and from there infer the history of mass loss from the central YSO.

2.1. CO SPECTROSCOPY

The low dipole moment of CO ($\sim$ 0.1 Debye) makes this molecule easily excited and often thermalized in many astronomical situations. For this reason, a measurement of the CO excitation provides an excellent estimate of the gas kinetic temperature. To achieve this, the line ratio R between the intensity of two rotational lines (e.g., J=2–1 and J=1–0) is often used. If the CO emission is optically thin, and the filling factor and the excitation temperature are the same for both transitions, R_{21}= 4 exp($-$11/T$_{ex}$), and a measurement of R gives directly an estimate of T$_{ex}$. Figure 3 (left panel, upper curve) shows a plot of R_{21} as a function of T$_{ex}$, illustrating how the optically thin line ratio increases quickly with excitation temperature from T$_{ex}$= 1 to 50 K, and tends monotonically to a value R=4 when T$_{ex}$ tends to infinity.

If the CO emission is extremely optically thick, the intensity ratio adopts the form R = [exp(5.5/T$_{ex}$)$-$1]/[exp(11/T$_{ex}$)$-$1], so it remains $<$ 1 for all values of the excitation temperature (Figure 3 left panel, lower curve); a measure of $R > 1$, therefore, indicates that the emission is not fully optically thick. In the intermediate case, the optical depth of the CO emission needs

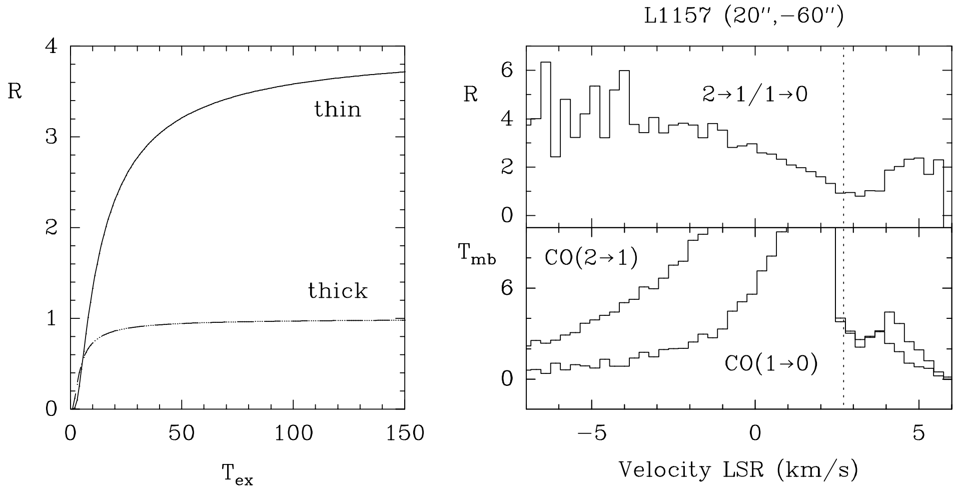

Figure 3. Analysis of the 2–1/1–0 CO line intensity ratio, R. Left.- R as a function of excitation temperature in the optically thin and thick limits. Right.- The bottom panel shows the CO 2–1 and 1–0 spectra (convolved to the same resolution) towards a position in the L1157 outflow. The upper panel shows the line intensity ratio R across the line profile. Note that R increases from a value of $\sim$1 (typical of thick emission) in the inner wings to a value of $\sim$4 (typical of thin emission) at high velocities.

to be estimated, or a rare CO isotope used to calculate the ratio. For many outflows, the the line ratio R changes with position, and for a given position, it depends on velocity. Figure 3 (right panel) shows CO 2–1 and 1–0 spectra toward the L1157 outflow together with the ratio R_{21} as a function of velocity. R increases monotonically with velocity, indicating that the emission is thinner at higher velocities, probably because the amount of gas flowing at high velocities is much smaller than that flowing at low speeds.

To estimate the CO optical depth, lines from different isotopes should be observed. If both J=1–0 lines of ^{13}CO and ^{12}CO (CO hereafter) are optically thin, for example, the CO/^{13}CO J=1–0 intensity ratio r is given by the abundance ratio $r = x(CO)/x(^{13}CO) \sim 90$. If the 1–0 line of ^{12}CO (the main isotope) is optically thick, however, the ratio will be $r \sim 90/\tau(\mathrm{CO})$. Thus, if the intensity ratio r is found to be significantly lower than 90, we can conclude that the CO 1-0 line is optically thick. This is actually the case in many outflows, but again r changes with the position in the outflow and the considered velocity range.

2.2. OUTFLOW PHYSICAL PARAMETERS

From observations of two lines of CO and one line of ^{13}CO it is thus possible to estimate the excitation temperature and the opacity of the outflowing gas.

Then, it is possible to estimate the gas column densities using the standard equations of the radiation transfer and opacity (see e.g. Margulis & Lada 1985, Levreault 1988). The mass of the outflowing material can thus be calculated by assuming a CO/H_2 abundance ratio. Finally, it is possible to study the distribution of mass with the line-of-sight velocity, and estimate in this way the momentum, the kinematic energy, and the mechanical power of the outflow. All these estimates are subject to important uncertainties, like the ambiguity separating at low velocities the outflow gas from the ambient material, as outflow wings tend to merge continuously with the ambient cloud component in the spectrum.

Another source of uncertainty is our ignorance of the angle the outflow axis makes with the plane of the sky, which is necessary to convert the observed velocity radial component into the three-dimensional velocity field. One approach is to model the shape and velocity field of the outflow lobes to obtain synthetic maps for comparison with the observations. Interesting attempts in this direction have been done by using conical and paraboloidal lobe geometries (e.g. Cabrit & Bertout 1986, 1990; Cabrit et al. 1988; Meyers-Rice & Lada 1991). One important application of this technique consists of simulating the observation of a model outflow and comparing the estimated parameters with the real ones. Doing this, Cabrit & Bertout (1990) show that the most accurate methods can estimate the outflow mass within a factor of 2, the momentum within a factor of 10, the flow force within a factor of 10, and the mechanical power within a factor of 60.

Despite the large uncertainties involved, CO spectroscopy is still the best method to obtain the physical parameters of bipolar molecular outflows. From the considerable efforts devoted during these last 20 years to extensive CO mapping, we know that flow sizes range from less than 0.1 pc to several pc. The observed (unprojected) terminal velocities range from a few $\mathrm{km\,s^{-1}}$ to about 100 $\mathrm{km\,s^{-1}}$, the kinematical time-scale (i.e., the flow length divided by the terminal velocity) ranges from about 10^3 yr to about 10^5 yr. The total molecular mass of the outflowing material ranges from a few $10^{-2}\,M_\odot$ to several hundreds $M_\odot$.

2.3. OUTFLOW CLUMPINESS

Multiline observations of CO and ^{13}CO in a number of bipolar outflows have shown that, in many sources, the high-velocity CO emission is optically thick (e.g. Bally 1982; Plambeck et al. 1983; Snell et al. 1984). For instance, the optical depths of both the CO 1–0 and 2–1 transitions in NGC 2071 and in S 140 are greater than 3 over a velocity range of ~ 30 $\mathrm{km\,s^{-1}}$ (Snell et al. 1984). On the other hand, the excitation temperatures of these transitions are ~ 12 K in both sources, and should equal the gas kinetic temperature, since the CO lines should be thermalized by collisions. As the observed antenna temperatures in the CO wings are considerably weaker than 12 K, one must conclude that the high-velocity emission arises in a clumpy gas which does not uniformly fill the telescope beam.

Plambeck et al. (1983) derived typical values of the filling factor of 0.1–0.2 in several molecular outflows, and Snell et al. (1984) found that the filling factor increases to nearly unity at the lowest outflow velocities. If the clump size distribution is independent of velocity, this means that there are many more clumps moving at low velocities than at high velocities; or, alternatively, that the smaller clumps move at higher velocities than the larger (more massive) ones.

Further evidence for the presence of clumping in the high-velocity gas has been provided by direct observations with high angular resolution. Tafalla et al. (1994) observed a striking clumped structure in the MonR2 outflow via CS observations: the flow clumps were found to be as dense as the ambient cloud (few $10^5 \mathrm{cm}^{-3}$), and to contain several solar masses each. They concluded that most of the outflowing gas -if not all- is in the form of dense clumps. Further direct evidence for clumpiness in other outflows was provided by Wootten et al. (1984), Avery et al. (1990), Garden et al. (1991), and Kitamura et al. (1990, 1992), among others.

3. Properties of Classical CO Outflows

In sections 3 and 4 we discuss separately the properties of "classical" and "highly collimated" outflows. Although the separation of outflows into these two categories is not absolute because outflows of very different collimation have been found over many years of research, there seems to be a clear dichotomy between outflows found during the 80's, which were bipolar but poorly collimated ("classical") and some extremely collimated outflows identified in the 90's. Such a dichotomy is not the result of just resolving better already known outflows, but represents the existence of a small population of extremely well collimated outflows, only found after the advent of the latest generation of radio telescopes (e.g., IRAM 30m, JCMT).

The properties of classical outflows have been the topic of several excellent reviews (e.g., Lada 1985, Snell 1987), and here we only attempt to enumerate them briefly, referring the reader to those papers for further details. Most of these properties have been derived from CO observations using the techniques described in the previous section, although the application of different criteria by different authors (contribution of low velocity gas, different inclination correction methods, etc) makes sometimes difficult to compare outflow properties from different authors. A systematic study of the outflow phenomenon using the currently achievable high spatial resolution and applying an homogeneous method of analysis is still an overdue piece of research.

3.1. OUTFLOW GEOMETRY

The most characteristic property of outflows is their bipolarity, which arises from the presence of two separated lobes of gas, one red shifted and the other blue shifted, with a young stellar object in between (Figures 1,2). An early question in outflow research was whether bipolarity is intrinsic or it arises from external, large-scale collimation. Although extended (tenths of parsec) structures of dense gas elongated perpendicular to the flow axis ("toroids") were found in many cases (Cantó et al. 1981; Torrelles et al. 1983), it is now believed that they represent more the effect of core disruption than a collimating agent (see below). Modern high resolution observations of molecular outflows reveal that the scale at which collimation occurs can be very small ($<$ 1000 AU for L1448, Guilloteau et al. 1992; HH211, Gueth & Gulloteau 1999), so if bipolarity is not fully intrinsic, it is associated with much smaller scales than initially thought.

To quantify outflow bipolarity, one usually defines the collimation factor R_{coll}, the ratio between the major and minor axes of the flow. This collimation factor depends on telescope angular resolution (see a nice graphic example in Snell 1987), so some care has to be exerted when using low resolution data to determine it. Figure 4 (left panel) presents a histogram of collimation factors for a sample of 26 outflows from Lada (1985), showing a wide distribution of R_{coll} values and an overabundance of systems with low collimation. This distribution implies that most outflows are poorly collimated, and that the observations cannot be explained simply from orientation effects in a sample of highly collimated outflows (Bally & Lada 1983). Different outflows must have different collimation factors, and on average, classical outflows are poorly collimated.

An important aspect of outflow morphology is the spatial distribution of the gas inside the lobes. Not many outflows have been mapped with the necessary angular resolution to study such distribution in detail, but in several cases where this has been possible, shell geometries have been found. L1551 is the classical example of a shell distribution (Moriarty-Schieven & Snell 1988, see also Figure 5), but it is by no means the only example (e.g.: NGC2071, Moriarty-Schieven et al. 1989; MonR2: Meyers-Rice & Lada 1991, Tafalla et al. 1997). In L1551, the shell surrounds a cavity devoid of molecular gas that can be seen as a hole in ^{13}CO maps (Moriarty-Schieven & Snell 1988) and as an optical reflection nebula in optical images (Graham & Heyer 1990). Such a combination of outflow shell and empty cavity strongly suggests that the outflow material represents ambient gas set into motion by an

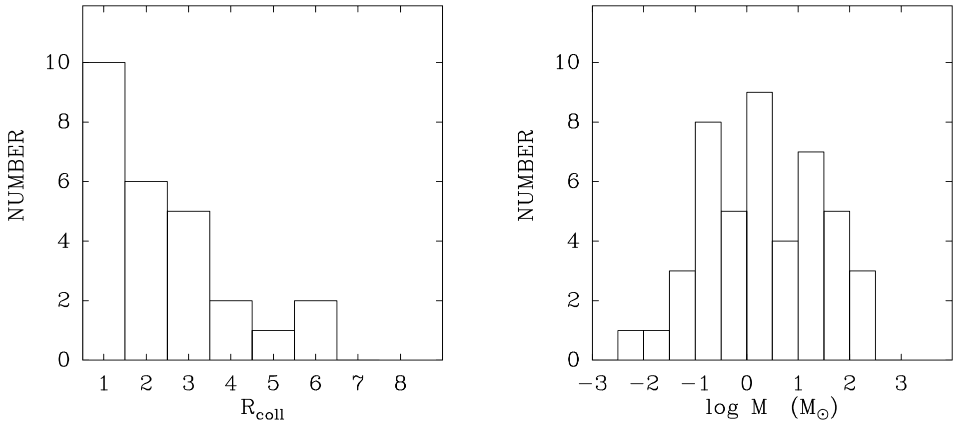

Figure 4. Right: histogram of the outflow collimation factor R_{coll} for a sample of 26 outflows, from Lada (1985). The large number of low collimation factors argues against a population of equally collimated outflows whose only difference is the orientation in the plane of the sky. Right: histogram of outflow masses for a sample of 46 outflows, from Snell (1987). The large values at the high end of the distribution can only result from the acceleration of ambient molecular material.

(invisible) wind from the central young stellar object. Whether the situation of L1551 applies to other (classical) outflows is not clear yet, as the sample of outflows studed in high detail is small, but the presence of cometary reflection nebulae in many objects (e.g.: Staude & Elsässer 1993) suggests a common pattern. We will return to this point and its implications for outflow evolution in Section 5.

Although bipolarity is the norm in outflows, deviations from this behavior are known to exist. A case of interest is that of quadrupolar outflows, which consist of four lobes of accelerated material, two of them red and two of the blue (e.g.: L723, Moriarty-Schieven & Snell 1989, Avery et al. 1990). The most likely explanation for these systems is the that they consist of a superposition of two independent outflows, each of them bipolar itself and, in fact, multiple YSOs are often found at the center of these outflows (in the case of L723 see Anglada et al. 1991). Source multiplicity should not be surprising given that a large fraction of stars seem to be born in binaries or small groups (Mathieu 1994). A recent NIR survey by Hodapp (1994) has shown that at least one third of all known bipolar outflows are associated with clusters of young stars. The fact that simple bipolar flows are seen suggests that the outflow phase may last much less than the total star formation period in the cluster, and that outflows are lit one or just a few at a time.

3.2. PHYSICAL PROPERTIES AND KINEMATICS OF THE OUTFLOW GAS

We have seen that the distribution of CO in outflows like L1551 suggests that most of the outflow material consists of swept up ambient gas. A stronger argument in this direction comes from the estimate of outflow masses, and this is illustrated in Figure 4 (right panel) with a histogram of the distribution of those masses in a sample of 46 objects (from Snell 1987). The large values seen at the high end of the distribution (> 10 M$_\odot$) cannot arise from the material being a direct ejection from the central YSO, and the only possible source of this gas is the surrounding ambient cloud. This implies that a driving agent accelerates molecular cloud material and gives rise to the observed CO lobes. The nature of this driving agent is still a mystery, and current outflow research consists mostly of an attempt to derive properties of this agent from the observed molecular material. Current ideas on this topic will be discussed in Section 7.

Despite the acceleration to supersonic velocities that the molecular gas has suffered, the physical properties of the gas in classical outflows do not significantly differ from those of the ambient cloud. Snell et al. (1984), for example, have shown that the kinetic temperature in the outflow gas is usually similar to that of the ambient cloud, if not even slightly lower. This does not mean that shocks do not occur in classical outflows, as there is plenty of evidence for them from IR and optical emission (Hodapp 1994; Reipurth, this volume), but that most of the gas we see in CO arises from material that has have enough time to cool down after it was accelerated to supersonic speeds. Less conclusive, on the other hand, have been attempts to determine the density and chemical composition of classical outflows. For most systems, these parameters are probably similar to those of the ambient gas.

From the point of view of kinematics, one of the simplest parameters one can determine in an outflow is the so-called kinematical age, which is the ratio between the outflow length and its total velocity extent (measured to some intensity threshold). Perhaps the most complete study of this parameter is due to Levreault (1988), who calculated kinematical ages for 25 outflows selected optically (i.e, probably rather evolved). This author finds that most systems have kinematical ages in the range 2-5 $\times 10^4$ yr, which is consistent with determinations by other other authors for different types of outflows. Such low kinematical ages, however, are probably not representative of the duration of the outflow phase by almost an order of magnitude. In fact, outflow statistics suggest that the outflow phenomenon lasts about 2×10^5 yr (Parker et al. 1991).

In addition to the outflow velocity extent, the spatial distribution of the gas at different velocities offers an important clue to the acceleration mech-

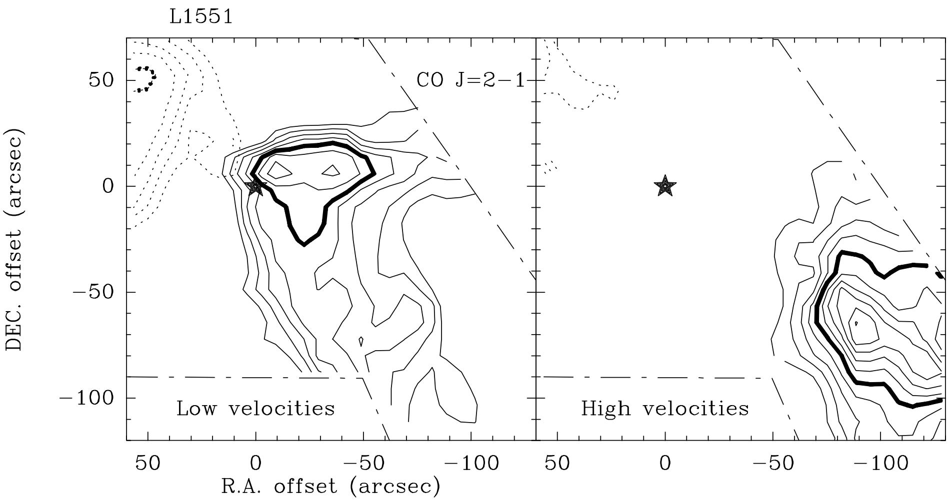

Figure 5. CO J=2–1 emission from the central region of the L1551 outflow observed with $\sim 12''$ resolution (Bachiller & Tafalla, 1994, unpublished data). The left panel shows the lowest velocity gas and the right panel shows the highest velocity emission detected. Note the shell-like distribution at low velocities and how the fastest gas appears far away from the central source and concentrated towards the outflow axis.

anism. Snell et al. (1984) have studied the centroid of the high velocity CO emission in outflows and have found that in some cases, the highest velocities are not reached near the YSO but at some distance from it. In L1551, this behavior appears as a systematic change in the position of the shells with velocity: as the velocity increases, the shells lie further from the outflow source and closer to the outflow axis (Moriarty-Schieven & Snell 1988). More generally, position-velocity diagrams of the CO emission from outflows sometimes show a quasi-linear increase of the terminal velocity with distance to the exciting source, in a pattern which has been referred as a "Hubble-like" law (Meyers-Rice & Lada 1991). Such a pattern could arise from a real linear increase of the outflow velocity with distance (e.g., Meyers-Rice & Lada 1991), although this does not necessarily mean that the driving wind really accelerates as it moves away from the YSO. The combination of momentum conservation and a density decrease away from the outflow source can explain such a pattern (Shu et al. 1991).

A more difficult parameter to determine is the exact direction of motion of the outflow gas. Meyers-Rice & Lada (1991), from modeling outflow position-velocity diagrams, conclude that the flow has to be rather parallel to the axis if one is to reproduce the observed CO patterns. The lack of a significant component of the outflow velocity field perpendicular to the outflow axis strongly argues against energy driven outflows, which would produce large inflating bubbles. Outflow acceleration must therefore occur by momentum conservation between a stellar wind/jet and the ambient gas (see also Masson & Chernin 1993).

3.3. OUTFLOW ENERGETICS

Bipolar outflows, as we have seen, consist of large masses of ambient gas moving at supersonic velocities. They therefore represent an important deposition of energy and momentum by a newly born star on its surrounding material. Quantifying the amount of this deposition is of great interest when studying the evolution of molecular clouds after star formation has occurred.

In their classical systematic study of the outflow phenomenon, Bally & Lada (1983) found a correlation between the bolometric luminosity of the exciting object and the rate of momentum and energy injection into the outflow. Figure 6 presents a modern version of this correlation (due to Cabrit & Bertout 1992), showing a systematic behavior extending over five orders of magnitude in source luminosity. This continuity in the trend strongly suggests that a single mechanism is responsible for the production of molecular outflows from both low and high mass stars.

As mentioned before, energy is probably not conserved during outflow acceleration (it is radiated away), so the amount of this parameter in the molecular material is not necessarily a good indicator of the energy content in the driving agent. Linear momentum, on the other hand, is most likely conserved, so the momentum in the CO outflow must equal the momentum in the invisible agent. As Figure 6 shows (left panel), outflow momentum exceeds photon momentum in the stellar radiation field by about two orders of magnitude. This means that unless stellar photons are scattered hundreds of times by the outflow material (extremely unlikely), outflow acceleration cannot be due to radiation pressure (Bally & Lada 1983).

The outflow gas is accelerated ambient material, so energies and momenta measured from CO data represent amounts already deposited on molecular clouds. Even for the weakest outflows (from low mass stars), kinetic energies are of the same order of the binding energies of the cores where the exciting source is formed, so outflow-core interaction can be an important element in core dispersal (Myers et al. 1988). Direct evidence for this interaction comes from the CO maps of outflows. As mentioned before, the L1551 outflow has evacuated a large cavity in its parent cloud by setting into motion a large amount of gas (Moriarty-Schieven & Snell 1988). Similar effects have been observed in many other systems, like NGC 2071 (Moriarty-Schieven et al. 1989), L43 (Mathieu et al. 1988, Bence et al. 1998), and Mon R2 (Wolf et al. 1990; Meyers-Rice & Lada 1991, Tafalla et al. 1997). Bipolar outflows, therefore, constitute a likely mechanism by which newly born stars disperse their parental environment and make the transition from embedded object

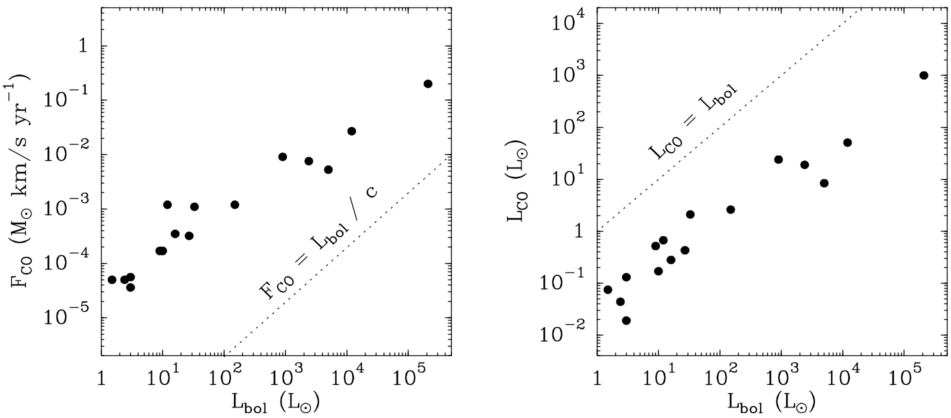

Figure 6. Correlation of outflow momentum flux (left) and mechanical luminosity (right) with source bolometric luminosity for a sample of bipolar outflows (from Cabrit & Bertout 1992). Note that the momentum flux in an outflow exceeds the YSO photon flux by almost two orders of magnitude. Bipolar outflows cannot be driven by stellar radiation pressure.

to visible star. It may even be possible that through the outflow mechanism a star is able to stop gravitational collapse and put an end to its formation phase, setting in this way its final mass (Shu et al. 1987; Velusamy & Langer 1998).

4. Properties of Highly Collimated CO Outflows

The first highly collimated outflows were identified in the early 90's thanks to the new generation of high resolution mm radio telescopes (Bachiller et al. 1990, Masson et al. 1990, André et al. 1990), and they were quickly interpreted as representing a previously missing stage of outflow life. Their discovery has been followed by a very intense search of additional examples, and during the rest of the 90's a sizable sample of collimated outflows have been built. Well known members of this outflow class include L1448 (Bachiller et al. 1990; Fig. 8), VLA 1623 (André et al. 1990), IRAS03282+3035 (Bachiller et al. 1991b), Orion B (Richer et al. 1992) HH211 (McCaughrean et al. 1994; Gueth & Guilloteau 1999; Fig. 7), NGC 2264G (Lada & Fich 1996), HH212 (Zinnecker et al. 1998), and SVS13B (Bachiller et al. 1998). In this section, we review the main properties of these highly collimated outflows, except for the heating and chemical anomalies recently found in some objects, that because of the large amount of recent results deserve a separate treatment and are discussed in Section 6. Previous reviews of the properties of highly collimated outflows can be found in Bachiller & Gómez-González (1992), Masson & Chernin (1993), and Bachiller (1996).

4.1. GEOMETRY AND COLLIMATION

High collimation is the main characteristic of this outflow class, although no clear-cut minimum value of R_{coll} has been set for an outflow to be classified as highly collimated. Values larger than 10 are easily achieved, and in some cases R_{coll} factors as high as 20 and 30 can be measured at high velocities (Richer et al. 1992, Lada & Fich 1996, Gueth & Guilloteau 1999). In most outflows collimation increases systematically with velocity, and the fastest gas lies close to the outflow axis and has the highest bipolarity. This seems a continuation of the trend found in the classical outflows (like L1551), but at speeds and R_{coll} factors that are about an order of magnitude higher.

The high bipolarity of some molecular outflows rivals the strong collimation seen in optical jets, and this has revived the idea that the relation between jets and outflows may be one of cause and effect (e.g. Masson & Chernin 1993), and not just represent two parallel phenomena having different origins (e.g. Mundt et al. 1987). To this end, it has been crucial the realization that optical jets are mostly neutral (few percent ionized, see Raga et al. 1990, Hartigan et al. 1994) and that the outflow phenomenon is much longer lived than initially thought (Parker et al. 1991), so stellar jets can potentially inject in the surrounding medium amounts of kinetic energy and linear momentum comparable to those observed in molecular outflows (Masson & Chernin 1993). In section 7 we will discuss with detail how these recent results have affected theoretical models of the outflow phenomenon.

Although the most collimated outflows look very much jet-like at the highest velocities, their behavior is much more classical at lower speeds. Figure 7 illustrates the behavior of HH211 (Gueth & Guilloteau 1999), one of the best collimated outflows known to date, which still shows a shell-like gas distribution at the lowest velocities (see top panel). Similar behavior has been observed in Orion B (Richer et al. 1992), L1448 (Bachiller et al. 1995), NGC 2264G (Lada & Fich 1996), and L1157 (Gueth et al. 1996, 1997), and may also be present in other highly collimated flows not studied yet with high enough angular resolution. In the cases of L1157 and HH211, the shells diverge away from the central source but converge at the end of the lobe, where strong H_2 (shocked) emission is observed. Bow shock models of this emission reproduce the main observed shapes (Gueth et al. 1996, Gueth & Guilloteau 1999).

4.2. KINEMATICS AND ENERGETICS

Highly collimated molecular outflows tend to have, in addition to a "classical" component, a fraction of extremely high velocity (EHV) gas moving at much higher speeds than those seen in classical outflows. In L1448, for example, terminal velocities are about 70 $\mathrm{km\,s^{-1}}$ for both lobes (Bachiller et

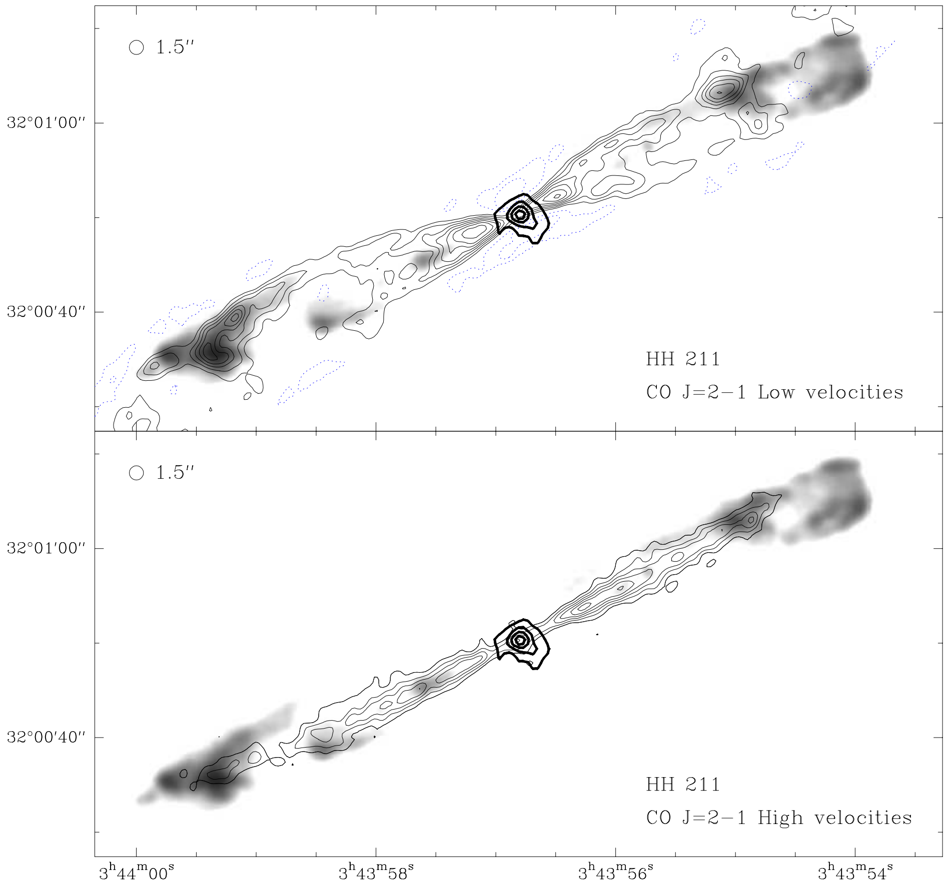

Figure 7. The highly collimated HH211 outflow in IC348 (from Gueth & Guilloteau 1999). Thin contours represent the CO 2–1 emission integrated in two different velocity intervals (low velocity on the top and high velocity on the bottom). Grey scale represents the H_2 v=1-0 S(1) emission. Thick contours are λ 1.3 mm continuum emission from the protostellar condensation HH211-mm.

al. 1990), and in HH7-11 (probably the record holder), molecular gas up to 150 $\mathrm{km\,s^{-1}}$ (with respect to the ambient cloud) has been found (Bachiller & Cernicharo 1990, Masson et al. 1990, Koo 1990). These observed velocities have to be corrected for projection effects, which are likely to be important given the the small angle with the plane of the sky that some highly collimated outflows seem to make. The resulting corrected velocities are among the highest observed in molecular gas.

In many highly collimated outflows, the EHV component appears forming discrete condensations often referred as molecular "bullets." Figure 8 illustrates the case of L1448, where the "bullets" are very well defined in position and velocity, and lie almost symmetrically located at each side of the exciting source (see also Guilloteau et al. 1992; Dutrey et al. 1997). Other sources with bullets include HH7-11 (Masson et al. 1990, Bachiller & Cernicharo 1990), VLA16293 (André et al. 1990), Orion B (Richer et al. 1992), IRAS03282+3035 (Bachiller et al. 1991b), IRAS2005+2720 (Bachiller et al. 1995), and HH111 (Cernicharo & Reipurth 1996, Nagar et al. 1997). From CO observations, the bullets are estimated to have typical sizes of a few 10^{-2} pc and typical masses of a few $10^{-4}\,M_\odot$ (Bachiller et al. 1990). Their kinematic time scales range from a few 10^2 to a few 10^3 yr.

In cases like L1448 and IRAS03282+3035, the terminal velocity of the EHV gas (bullets) decreases with distance from the outflow origin, while the terminal velocity of the low-velocity outflow increases according to an approximate "Hubble-like" law. This behavior suggests that the EHV jet-like component could be injecting momentum into the ambient gas to produce the lower velocity outflow, and in fact, the EHV gas sometimes contains amounts of energy and momentum comparable to those of the lower velocity outflow (Bachiller et al. 1990, 1991b). Whether the EHV gas is in fact the driving agent of the outflow or a manifestation of a hidden wind will be further discussed in Section 7 in the context of outflow models.

The physical origin of the molecular bullets is still subject to debate. Bachiller et al. (1990) interpreted them as coherently moving pieces of gas ejected from the immediate vicinity of the central YSO. Richer et al. (1992) have argued that given the internal velocity dispersion of the bullets ($\sim$ 6 km s^{-1} in L1448), if they were ballistic pieces of gas, they should expand and dissolve as they move away from the YSO, so either they are somehow confined or they are produced in situ, most likely through some type of flow instability. Chernin et al. (1994), from numerical simulations, produce features similar to the observed bullets by reformation of molecules in post-shock gas. Although it is not clear which of these interpretations is correct, an interesting clue to their origin comes from the symmetrical location of bullets in both position and velocity with respect to the central source (at least in L1448, Bachiller et al. 1990; IRAS03282+3035, Bachiller et al. 1991b; HH111, Cernicharo & Reipurth 1996). This symmetry implies that there are pairs of bullets, one of them red and the other one blue, which have the same kinematical age and probably a related origin. This is best understood if there is some type of instability in the central source that gives rise to quasi-periodic ejections every $10^2 - 10^3$ yr. Whether all outflow material is ejected during these outbursts and whether the bullets represent ejected component or ambient gas excited by the ejection are still mysteries that need to be solved. In any case, the bullets illustrate the violent and non steady nature

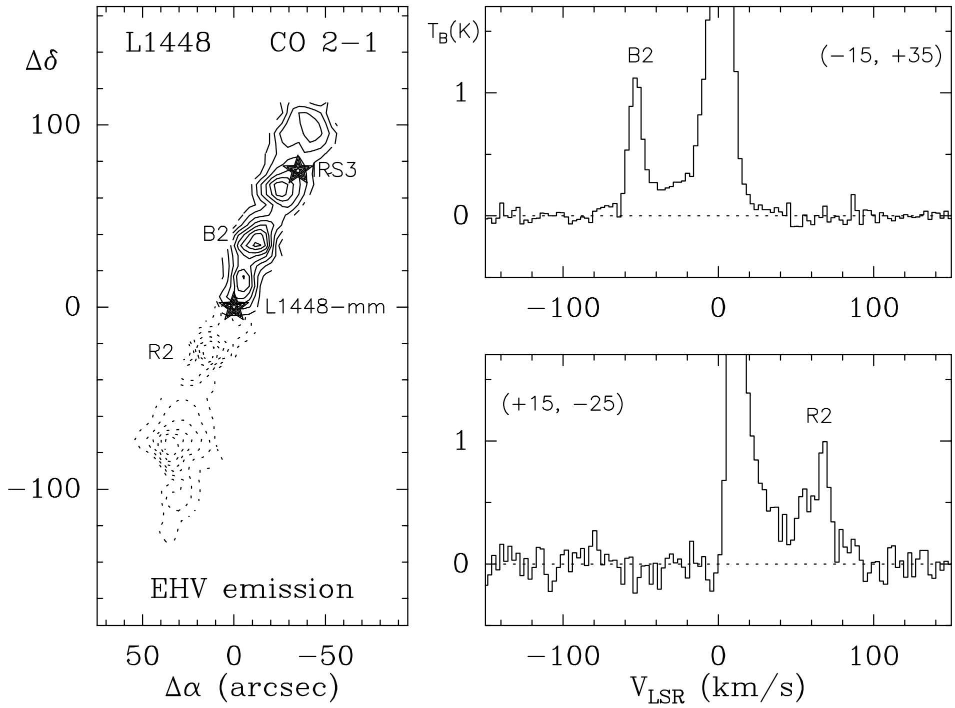

Figure 8. CO 2–1 emission in the L1448 outflow (from Bachiller et al. 1990). The left panel shows the EHV component of the outflow. Solid contours represent blue shifted emission in an interval of 30 km s^{-1} wide centered at –50 km s^{-1} from the ambient velocity. Dashed contours are for red shifted emission in a similar interval centered at +50 km s^{-1} from the ambient velocity. Note the presence of high-velocity molecular "bullets" along the jet axis. The CO spectra obtained toward the positions of bullets B2 and R2 are shown in the right panels. Position offsets are in arcseconds with respect to the position of the Class 0 source L1448-mm.

of the outflow phenomenon.

Overall, highly collimated outflows are more energetic than classical flows from sources of comparable luminosity. This is not just due to the presence of an EHV component, although the EHV gas makes a substantial contribution to the outflow energy and momentum (40% and 60%, respectively for IRAS03282+3035) despite constituting a small fraction of the total mass (20% in IRAS03282+3035). This systematic higher energy and momentum content of the highly collimated outflows is nicely illustrated in the recent study by Bontemps et al. (1996). These authors have analyzed a sample of 45 low-mass, nearby outflows both from Class 0 sources (highly collimated) and from Class I YSOs (classical), and in Figure 9 we present their plot of outflow momentum flux versus source bolometric luminosity in a similar manner than was presented for classical outflows in Figure 6. In

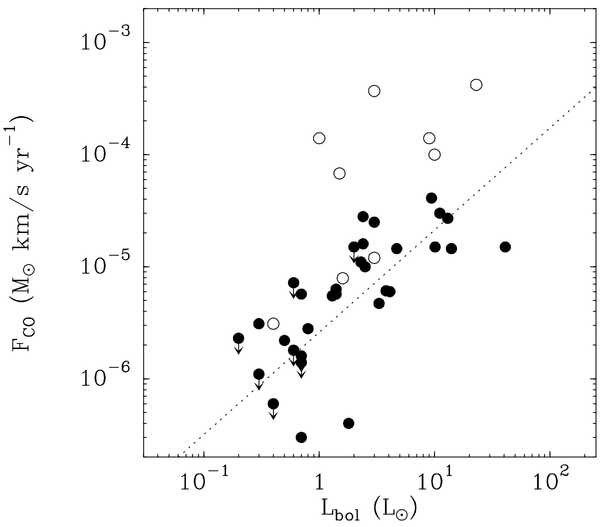

Figure 9. CO momentum flux F_{CO} versus bolometric luminosity L_{bol} for 41 young stellar objects (Bontemps et al. 1996 data). Class 0 and Class I sources are represented as open and filled circles, respectively. The dashed line represents the "best fit" correlation found only for Class I sources. Note that all Class 0 sources lie well above this line.

agreement with Bally & Lada (1983) (also Cabrit & Bertout 1992), classical outflows follow a linear relation between momentum flux and source luminosity. Highly collimated outflows, on the other hand, have systematically an order of magnitude more momentum than classical sources of equal luminosity, and this suggests that the exciting sources of these outflows are losing mass in a more violent manner than the sources of the classical flows. The origin of this energy excess, and of the other extreme properties of the highly collimated outflows, constitutes one of the most intriguing aspects of outflow research, and in the next section we explore the possibility that it is related to the extreme youth of the outflow exciting sources.

5. Outflow Evolution

After reviewing in the last two sections the properties of classical and highly collimated outflows as derived from observations, we now take a more speculative approach and explore how the differences between these two types of outflows may be understood in terms of outflow evolution. This is a topic that has only begun to receive the attention it deserves (e.g., Padman 1997, André 1997), so many of the ideas we present here are still tentative and may be subject to change. Still, understanding how outflows evolve with time and how the observed properties depend on the outflow evolutionary status appears as the best strategy to organize a rather diverse and sometimes seemingly conflicting collection of observational results. It also offers the hope to clarify the still mysterious origin of bipolar flows.

One of the main obstacles when studying outflow evolution is the identification of a reliable time indicator, an internal clock that allows one to order outflows by age. Using outflow properties to set this clock may produce a circular argument when studying outflow evolution, so it seems preferable to use the properties of the central YSO as an age indicator. This has the additional advantage of having already a time sequence of YSO evolution in terms of discrete classes (Adams et al. 1987; Lada 1991; André et al. 1993), with an even finer subdivision in terms of the bolometric temperature (Myers & Ladd 1993). For the purposes of our discussion, the division into classes will suffice, as our arguments are still rather qualitative.

The first evidence for age being at the root of the differences between classical and highly collimated outflows comes from the different classes of the sources powering these two types of systems. Highly collimated outflows like L1448 (Fig. 8) and HH211 (Fig. 7) are powered by Class 0 objects, which are considered the youngest protostars known (André et al. 1993), while classical outflows like L1551 are excited by Class I YSOs, which represent a more evolved state.

5.1. CHANGES IN OUTFLOW COLLIMATION

Outflows from Class 0 YSOs like HH211 (Fig. 7) and L1448 (Fig 8) appear highly collimated, while outflows from Class I objects tend to be much less collimated. Even L1551 (Fig. 1), one of the most collimated classical outflows, is still different from the almost jet-like systems HH211 and L1448, both powered by Class 0 YSOs. This suggests that by the time a YSO reaches the Class I stage, its bipolar outflow has lost an appreciable part of its collimation. Molecular outflows, therefore, decollimate as they evolve, starting like highly bipolar systems and changing to classical flows.

Outflow decollimation seems accompanied by the opening of a cavity in the parent cloud. In HH211 (Fig. 7) and L1448 (Bachiller et al. 1995), this cavity is narrow and has straight walls, with an opening angle of about 30°, while in L1551 the cavity is much broader ($\sim 90°$) and has almost parabolic walls (Figs. 1 and 5). This is consistent with the outflow eroding the parent cloud, and opening a broader and broader channel as time passes. How exactly this process occurs is still a matter of debate. In the jet model of Masson & Chernin (1993), the jet "wanders" in angle, sweeping up different portions of the ambient cloud and therefore broadening with time. Raga & Cabrit (1993) have proposed that bow shocks give outflows their transversal dimension, so in this picture outflow broadening will imply bow shock broadening. Another possibility is that in addition to a highly collimated component, outflows also contain a broader wind. In this case, the jet component would dominate at early times because of its larger directivity, and the wider angle component would become apparent only later, perhaps because a central channel along the outflow has been opened.

5.2. CHANGES IN THE KINEMATICS AND ENERGETICS

Outflows from Class 0 sources have faster gas than outflows from Class I YSOs, so evidence points to a slowing down with time of the outflow material. This seems to occur by the weakening of the EHV component, which is already undetectable by the end of the Class 0 stage, while outflows from both classes have comparable amounts of slow moving gas. Outflows therefore evolve in time by increasing the relative fraction slow material with respect to fast moving gas, an idea previously proposed by Bally (1986) in the context of classical high mass outflows.

The above evolutionary scenario, however, seems to conflict with the work from Masson & Chernin (1992), who have studied the distribution of mass with velocity in several outflows. These authors find distributions with similar slopes, suggesting that the ratio between high and low velocity gas is common to all outflows. The contradiction between this result and our proposed evolutionary scenario is only apparent, and a more careful study of the distribution of mass with velocity shows so. In Figure 10 (adapted from Tafalla 1993) we present the distributions of outflow wing intensity with velocity for a sample of 6 outflows, including the data for L1551 and NGC2071 that Masson & Chernin used in their study. As the figure shows, all outflows have similar slopes at low velocities, with an average value of about -1.5, in agreement with Masson & Chernin (1992). At higher speeds, however, the slope of the distribution changes, becoming steeper and reaching values of the order of -4. Such a steepening in the gas distribution was first noticed by Kuiper et al. (1981) for the Orion outflow, and a nice recent example was presented by Lada & Fich (1996) for NGC 2264G. The outflows in Figure 10 have been ordered vertically by the velocity of the break point, which is largest in L1448 (≈ 30 $\mathrm{km\,s^{-1}}$) and smaller in Mon R2 (≈ 6 $\mathrm{km\,s^{-1}}$). This ordering, in addition, matches the ordering by kinematical age (Tafalla 1993) and agrees intuitively with the expected ordering of YSO age (note however, mixture of low and high mass objects). The solution to the kinematical evolution of outflows may therefore arise from the combination of a constant slope at low velocities and a systematic decrease in the fraction of high velocity gas, which makes the break point in the mass distribution move with time toward lower and lower velocities.

Additional evidence for the slowing down and weakening of outflows with time comes from the mentioned fact that young, highly collimated outflows

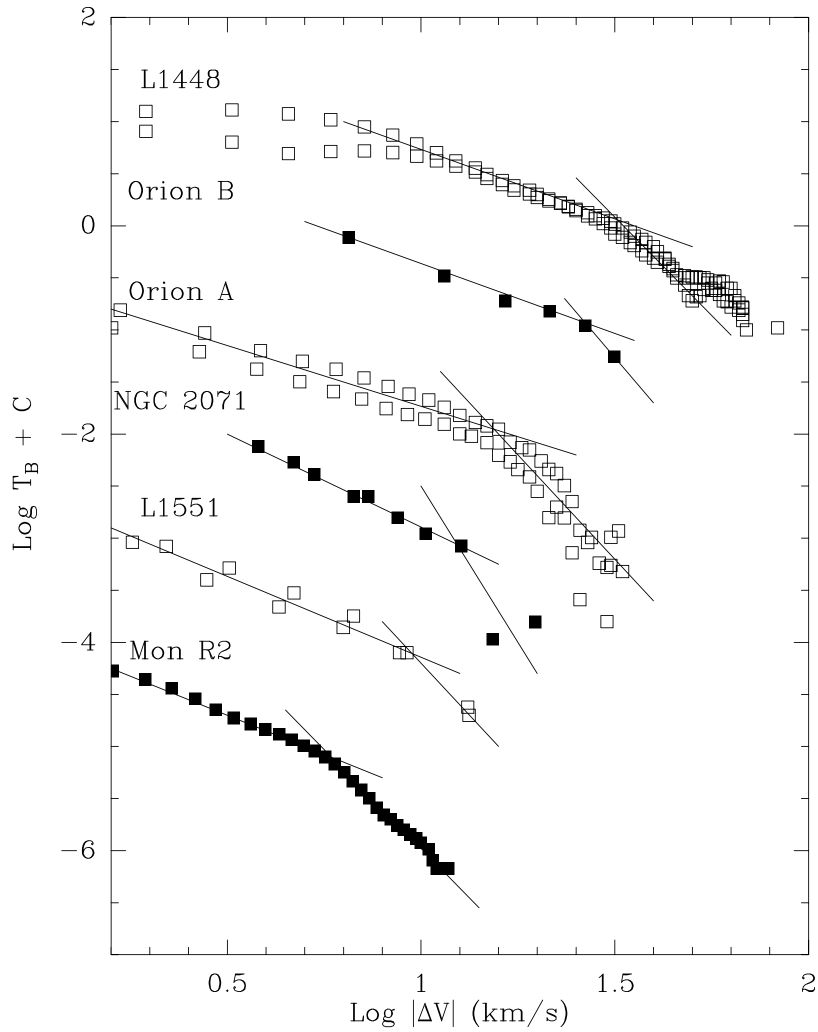

Figure 10. Log-log brightness distribution with velocity for a series of outflows of different ages. Note that the point where the distributions changes slope moves to lower velocities from top to bottom of the figure. This change seems associated with an increase of the outflow age. Data from different authors compiled by Tafalla (1993).

are more energetic than classical flows (Section 4.2). The work of Bontemps et al. (1996) shows that there is a very good correlation between the outflow momentum flux and the amount of circumstellar mass, and this is illustrated in Figure 11 (see also Saraceno et al. 1996). As circumstellar mass is a likely indicator of age (mass decreases as age increases), the correlation in the Figure suggests again that outflow power decreases with time.

5.3. CHANGES IN THE PHYSICAL AND CHEMICAL CONDITIONS OF THE OUTFLOW GAS

As was mentioned in Section 4 and will be discussed in the next section, high velocity outflows present evidence for warm molecular gas and spectacular chemical anomalies. These features can be explained as the result of strong shocks in the outflow gas, something that is not found, at least with that magnitude in classical flows. High velocity outflows, therefore, seem to interact more strongly with the surrounding environment, and most of the signatures of such an interaction (like chemical anomalies) have vanished by the time an outflow appears as a classical flow. Whether such a decrease in the interaction occurs because of the gradual clearing of the outflow path or because of an intrinsic weakening of the driving wind is not clear yet, but the strength of these shock signatures seems a good indicator of the outflow age (Codella et al. 1999).

5.4. AN EMPIRICAL TIME SEQUENCE OF LOW-MASS OUTFLOWS

After reviewing the fragmentary evidence for outflow evolution and discussing how observations suggest a transition between different stages, we conclude this Section proposing an empirical time sequence of outflows. Given that most observations of extremely young outflows (Class 0) are restricted to low mass systems, we will also restrict ourselves to this type of outflows. Our purpose here is to present a time sequence based on well known outflows, with the implicit assumption that differences between them are due to their different evolutionary status.

• First stage, L1448 (also IRAS03282+3035). The molecular outflow is highly collimated, almost jet-like, with a large fraction of extremely high velocity gas. Molecular "bullets" appear as secondary components in the spectra at extreme velocities and in the maps they look like high velocity clumps. SiO abundance is anomalous by a large factor ($> 10^4$) with respect to quiescent gas. The powering source is an extremely embedded YSO not visible in the near IR (Class 0).

• Second stage, L1157 (also BHR 71). The outflow appears less collimated and its terminal velocity is lower than in the phase before. There is no evidence for "bullets" in the spectra, but the maps show regions with large amounts of warm ($\sim$ 100 K) gas (hot spots). Very strong abundance anomalies: molecules like SiO and CH_3OH produce lines with prominent wing components, characteristic of high excitation and high molecular abundance. Exciting source still invisible in the NIR (Class 0).

• Third stage, L1551 (also NGC 2071). The systematic decrease of collimation and terminal velocity continues. Clear shell structure surrounding an evacuated cavity with a reflection nebula. Optical Herbig-Haro objects

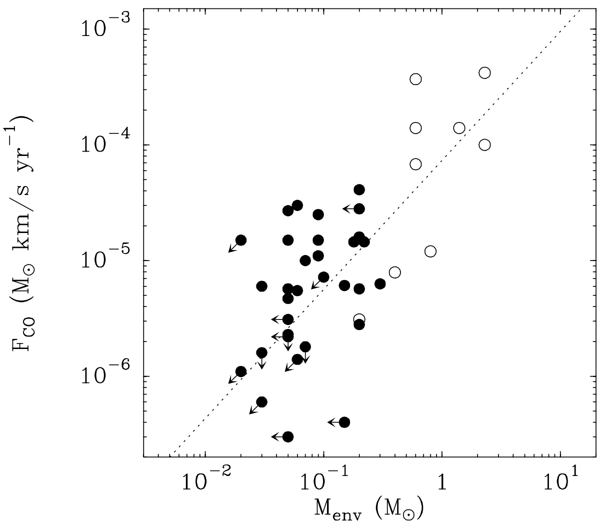

Figure 11. CO momentum flux F_{CO} versus circumstellar envelope mass M_{env} for 41 young stellar objects (Bontemps et al. 1996 data). Class 0 and Class I sources are represented as open and filled circles, respectively. The dashed line represents the "best fit" correlation for entire sample. Note that all Class 0 and Class I sources seem to follow the same correlation.

are visible. Large fraction of low velocity gas, which may appear in extreme cases forming detached wings in the CO spectra. Evidence for perturbation in the dense core and no chemical anomalies. Exciting source is Class I.

6. Shock Effects

Protostellar outflows are strongly supersonic, so they are expected to shock the surrounding cloud giving rise to rapid heating and chemical processing. In the more violent outflows, those from Class 0 protostars, these processes tend to be enhanced.

6.1. SHOCK HEATING

The molecular gas subjected to the passage of shocks is rapidly heated and then cools very rapidly ($<$ 100 yr) due to line radiation (e.g. Kaufman & Neufeld 1996). Different spectral lines can dominate the cooling process, depending on the temperature regime, and such lines will indeed be the best tracers to diagnose the cooling region. The importance of the dust emission is uncertain. For instance, IRAS detected diffuse far-IR emission from the shocked region in L1551 to be 18% of the bolometric luminosity of the central source (Edwards et al. 1986; Clark & Laurejis 1986), but it is not possible to estimate the possible contribution from spectral lines (e.g. H_2, CO) only with the IRAS data.

At temperatures up to ~5000 K, attained in regions subjected to dissociative J-shocks, the main coolant is the 63 μm line of [OI] (Hollenbach 1985). Observations with the KAO and ISO have allowed the measurement of this line in a handful of HH objects and outflows from Class 0 objects (Cohen et al. 1988, Ceccarelli et al. 1997, Saraceno et al. 1998). The [OI] line intensity, which is proportional to the mass flux into the J-shock, is correlated with the force of the CO flow F(CO) (Saraceno et al. 1998).

At temperatures around 2000 K the main coolants of the dense shocked regions are the vibrational near-IR lines of H_2 (Neufeld & Kaufman 1993). This temperature is typical of shocks with velocities 10–30 $\mathrm{km\,s^{-1}}$ (Shull & Beckwith 1982, Draine et al. 1983, Smith 1994). Indeed the v=1–0 S(1) line of H_2 at 2.122 μm is detected toward a high number of HH and CO outflows. The comprehensive survey by Hoddap (1994) shows that the H_2 emission adopts a variety of complex morphologies, with H_2 jet-like filaments and bow-shaped working surfaces being observed in a number of sources. The ratio of H_2 to the outflow power (estimated from CO) is observed to vary strongly from source to source (e.g. Davis & Eislöffel 1995), probably because of the combination of several factors such as extinction, H_2 emission decline due to cooling, and outflow power time variations.

At temperatures from 1000 K down to a few 100 K, the pure rotational lines of H_2 in the mid-IR, and the high-J (up to J~30) lines of CO in the far-IR are observed to be strong (e.g. Cabrit et al. 1998, Nisini et al. 1998). These temperatures are typical of slow shocks with velocities 10–25 $\mathrm{km\,s^{-1}}$ and densities around 10^5 $\mathrm{cm^{-3}}$.

Molecular lines of shock-enhanced species (e.g. NH_3, CH_3OH) trace chemically processed gas at temperatures as low as 60– 100 K (Bachiller et al. 1993, 1995; Tafalla & Bachiller 1995), which is nevertheless significantly hotter than the ambient gas (usually at 10– 20 K). This temperature regime seems to be particularly interesting for the chemical studies which are carried out at mm wavelengths.

6.2. SHOCK CHEMISTRY

The heating and compression caused by shocks often gives rise to dramatic effects in the chemical composition of the surrounding molecular cloud. Processes such as dissociation, endothermic reactions, sublimation of ices, and disruption of dust grains lead to a "shock-chemistry" which is radically different from that operating in the quiescent medium. Some of these processes are fast, and the cooling times of the shocked region are short, making the chemistry strongly time dependent.

Dissociative J-shocks destroy molecules in the resulting hot (~10^5 K) layer of shocked gas, but molecules can reform when the gas cools, or within the warm region around the hot layer. Such violent shocks can also destroy dust grains and produce thermal sputtering, resulting in the injection of refractory elements (e.g. Si and Fe) into the gas phase.

C-shocks, on the other hand, are particularly efficient at triggering a rich molecular chemistry, since they increase the temperature to moderate values (∼2000 K) in a thick layer where the molecules are preserved. Reactions that overcome energy barriers of a few 1000 K can proceed in such conditions, and in particular the very chemically active OH radical is formed by $O+H_2 \rightarrow OH+H$ (energy barrier of 3160 K). OH contributes to the formation of water by further reaction with H_2: $OH+H_2 \rightarrow H_2O+H$ (energy barrier of 1660 K). HS and H_2S are formed by similar reactions. Additionally, in C-shocks, non-thermal sputtering due to dust-molecule or to dust-dust collisions (Schilke et al. 1997, Caselli et al. 1997, Pineau des Forêts et al. 1997) results in the injection of refractory and volatile species, mainly from grain mantles, into the gas phase. The entrance of this material together with the presence of a high abundance of OH in the gas phase will produce oxides such as SO and SiO (see e.g. Bachiller 1997, van Dishoeck & Blake 1998, and references therein).

As the gas cools, reactions with high energy barriers will not be operative, and the chemistry will be dominated again by the usual low-temperature reactions. Depletion of molecules onto dust grains starts again to be important, reducing the abundances of some of the newly formed molecules (e.g. see the case of water, Bergin et al. 1998). Nevertheless, the chemical composition of both the gas and the solid phases will remain altered, keeping a memory of the passage of the shock wave.

Recent observations with high angular resolution and sensitivity are providing important insights in the shock-chemistry phenomena. Observations of the IRc2 outflow in Orion A have provided valuable information about the chemical processes induced in the surrounding medium by the formation of a high-mass star (Blake et al. 1987). But the cases of high-mass stars are particularly complex due to the confusion among different gas components along the line of sight.

The chemical effects of shocks are better studied in outflows from Class 0 sources because these are particularly energetic and highly collimated, so they contain shocked regions well separated spatially from the quiescent protostellar envelope. Recent studies of this type of outflows include NGC1333/IRAS4 (Blake et al. 1995), NGC1333/IRAS2 (Blake 1996, Langer et al. 1996, Bachiller et al. 1998), L1641-N (McMullin et al. 1994), HH25-MMS (Gibb & Davis 1998), and BHR-71 (Bourke et al. 1997; Garay et al. 1998). IRAS16293-2422 was studied in detail by Blake et al. (1994) and van Dishoeck et al. (1995), but only toward the position of the driving object.

6.3. OBSERVATIONS OF SHOCK CHEMISTRY IN L1157

A comprehensive chemical study including many different species has been recently carried out on the outflow from the Class 0 source L1157-mm (Bachiller & Pérez Gutierrez 1997). Due to its proximity (440 pc), high collimation, favorable orientation in the sky, and high column densities in the shocked region, L1157 appears as one of the best objects to study the rich phenomenology associated with young bipolar outflows.

The CO outflow in L 1157 (Umemoto et al. 1992; Bachiller & Pérez Gutiérrez 1997, Fig. 12) is driven by IRAS 20386+6751 (L1157-mm), a very cold source of about 11 $L_\odot$ embedded in a dense NH_3 core (Bachiller et al. 1993). The central source presents all the attributes of a Class 0 source, including a relatively strong millimeter flux due to thermal dust emission (Gueth et al. 1997). The mm-wave continuum emission consists of a compact ($\leq 1''$) source surrounded by spatially-extended, low-level emission which arises from the heated edges of the cavity excavated by the outflow. High-angular resolution images in the J=1–0 line of CO, ^{13}CO, and C^{18}O (Gueth et al. 1997) show that the C^{18}O emission is associated with the protostellar condensation, whereas the ^{13}CO line emission mostly originates from a extended envelope and the limb-brightened edges of the outflow; the CO line wings trace the bulk of the outflowing material. Possible gravitational infall is suggested by the self-reversed ^{13}CO profiles and the narrow C^{18}O lines.

The sharp increase of the CO brightness temperature towards the blue shifted lobe in L 1157 (Fig. 12) is attributed to gas heating produced by the shock. Multiline observations of ammonia, the best interstellar thermometer, confirm this interpretation, and provide a good estimate of the gas kinetic temperature in the shock, which results to be in the range 60– 100 K (Bachiller et al. 1993). The bow shocks at the head of the cavities are particularly bright in NH_3 (3,3), and VLA images from Tafalla & Bachiller (1995) reveal the hot regions of the bow shock structures seen in the high-velocity CO. The ammonia abundance can be estimated in both the quiescent gas and in the high-velocity outflow, and it results to be enhanced by at least a factor of 10 in the shocked region.

Bachiller & Pérez Gutiérrez (1997) have carried out a survey of the blue shifted lobe in L 1157 to study the chemical composition of the gas affected by the passage of the shock. About 50 different lines of 27 molecules (including rare isotopic species) were observed toward the central source and toward several positions with evidence for shock, in particular the two prominent NH_3 peaks of the blue shifted lobe: B1 at (20″, −60″), and B2 at (35″, −95″).

An immediate result from these observations is that some molecular species such as C_3H_2, N_2H^+, $H^{13}CO^+$, and DCO^+ are only observed toward the cold gas condensation around the exciting source, whereas some other

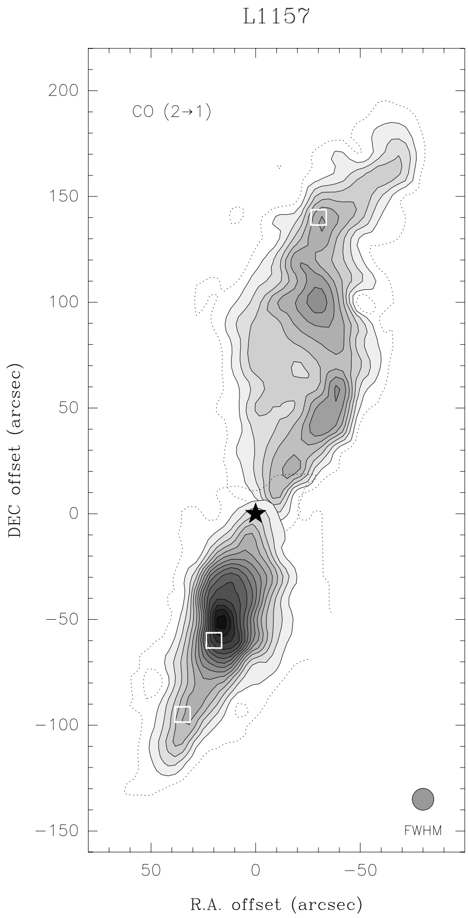

Figure 12. CO 2–1 emission from the L1157 outflow integrated over velocity intervals from −20 to 3 km s^{-1} (blue shifted gas to the south of the driving source) and from 3 to 30 km s^{-1} (red shifted gas toward the north). Position offsets are in arcsec with respect L 1157-mm, the outflow exciting source. First contour and step are 11 K km s^{-1}. The squares mark the positions of SiO emission peaks in which Bachiller & Pérez Gutiérrez (1997) carried out a survey of molecular lines.

molecules (such as SiO) only trace the warm gas in the shock. This result is important for studies of the structure of the central infalling condensation, since one can avoid the outflow contribution to the line profiles by observing the source vicinity in lines of C_3H_2, N_2H^+, $H^{13}CO^+$, and DCO^+. This does not mean that the outflowing gas is fully free of these molecules, but that the column densities are insufficient to produce significant wings in the profiles.

All the other detected molecules (SiO, CH_3OH, H_2CO, HCO^+, HCN, HNC, CN, SO, SO_2, CS) present emission in the outflow. The extreme case is SiO which is enhanced by a factor of $\sim 10^6$ (see also Mikami et al. 1992, Zhang et al. 1996, Avery & Chiao 1996). This is similar to what it is observed at the heads and along the axes of some other highly-collimated outflows (Bachiller et al. 1991a; Martín-Pintado et al. 1992; McMullin et al. 1994). The other molecular species with broad emission are observed to be enhanced by factors ranging from a few to a few hundred.

Figure 13 shows molecular line maps of the blueshifted lobe of L1157. There are important differences in the spatial distribution among the different species: some molecules such as HCO^+ and CN present their maxima close to the central source, while SO and SO_2 are brightest (in peak intensity) around the most distant shocks, with OCS presenting the most distant peak. Other molecules such as SiO, CS, CH_3OH, and H_2CO present an intermediate behavior. Such differences cannot be attributed solely to excitation conditions: an important gradient in chemical composition is observed along the outflow. It is very likely that this gradient is related to the strong time dependence of shock chemistry.

As an example of time dependence, consider the chemistry of SO, SO_2, and OCS, which has been recently modeled by Charnley (1997). It is believed that sulfur is released from grains in the form of H_2S, and that it is then oxidized to SO and SO_2 in a few 10^3 yr; the formation of OCS needs a few 10^4 yr. This is in agreement with the observations of L 1157, since the SO/H_2S and SO_2/H_2S ratios do increase with distance from the source (i.e. with time), and OCS emission in only observed in the most distant position (i.e the oldest shock).

Methanol (CH_3OH), with an abundance of a few percent, is thought to be the most abundant molecule in ices after water (Allamandola et al. 1992). Indeed, millimeter-wave observations of L 1157 show that the abundance of methanol is enhanced by a factor of 400 in the shock (Bachiller et al. 1995, Avery & Chiao 1996). There is increasing evidence that high abundances of methanol in gas phase are able to drive a chemistry completely different from the usual chemistry operating in dark clouds. In particular, laboratory experiments show that a significant fraction of the methanol released into the gas phase could produce H_2CO in a relatively short time (e.g. Bernstein et al. 1995). Solid formaldehyde (H_2CO) has also been recently discovered in the vicinity of protostars (Schutte et al. 1996), and our observations of L 1157 indicate that H_2CO in enhanced by a factor close to 100 in the shocked region. The chemistry of formaldehyde is probably closely related to that of methanol in both solid and gas phases.

Chemical studies provide a powerful tool to investigate the physical conditions of the shocked gas. As discussed above, NH_3 provides good estimates of the kinetic temperature. Once the temperature is known, multi line studies of SiO and CH_3OH provide reliable estimates of the volume densities. In the case of the L 1157 bow shocks, the density is found to be in excess of 10^6

L1157. Blue lobe.

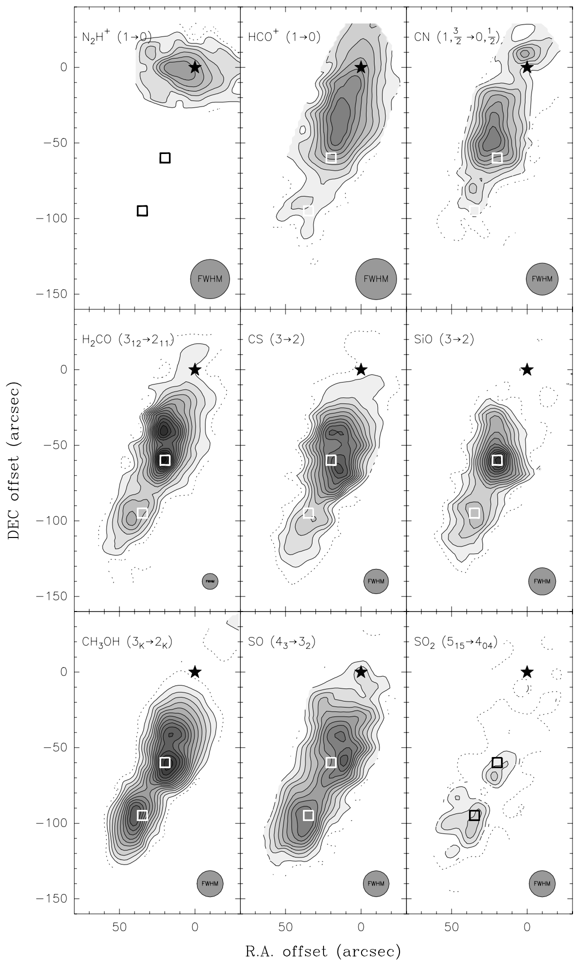

Figure 13. Maps of integrated intensity for different molecular lines in the blue shifted lobe of the L 1157 outflow obtained with the IRAM 30-m telescope. The white squares indicate the positions of the SiO emission peaks. Note the large differences observed in the distribution of the different molecules (see discussion in the text).

cm^{-3} (Bachiller et al. 1993, 1995).

7. Properties of the Primary Wind

If radiation pressure from the central YSO lacks enough momentum to drive a molecular outflow (Bally & Lada 1983, see also Section 3), a mechanical agent like a stellar wind seems the most likely responsible for this phenomenon. Despite many years of both observational and theoretical work, however, basic characteristics of this agent, like its composition and collimation, are still subject to strong debate, and different theories for the launching mechanism have been proposed. In this section, we review the status of this important topic, discussing both observational attempts to detect the outflow agent and theoretical models of outflow acceleration.

7.1. OBSERVATIONS

The driving wind could be either neutral or ionized, and if neutral, it could be either molecular or atomic. Depending on this state, its detection could be done at radio, infrared, or optical wavelengths.

If the driving agent is molecular, it could probably be detected using the same tracers used to detect molecular clouds: line emission from abundant species like CO. However, the molecular emission from an outflow comes mostly from swept-up ambient material (Section 3), so any possible driving wind contribution should be separated from the accelerated ambient component. As the driving wind should move faster than the swept up ambient gas, there is the possibility that the EHV component seen in highly collimated outflows represents the driving agent. If this were the case, however, classical outflows, which lack EHV component, would be either driven by an additional (invisible) agent, or they would have an undetected EHV component. Deep searches for EHV gas towards classical outflows have been carried out (Margulis & Snell 1989; Choi, Evans, & Jaffe 1993), but they have tended to concentrate on high mass outflows. For the case of L1551 (see Koo 1989), no clear evidence for a EHV component, despite the strong outflow signal at low velocities. It seems, therefore, that the EHV gas, although closely connected to the driving wind (may be recently accelerated), is not the agent of outflow acceleration. Deeper searches for a molecular driving wind component should be made to further explore this possibility.

If the driving wind is atomic, 21-cm HI emission could reveal its presence. In fact, HI observations have allowed the detection of a neutral component towards a few outflows, like NGC 2071 (Bally & Stark 1983), HH7-11 (Lizano et al. 1988, Rodríguez et al. 1990), and L1551 (Lizano et al. 1988, Giovanardi et al. 1992). The origin of this atomic component, however, has been interpreted differently by different authors: Bally & Snell (1983) propose it arises from the dissociation of ambient molecular hydrogen due to outflow shocks, while Lizano et al. (1988) propose the HI emission traces a wide-angle neutral wind from the central protostar. Unfortunately, the extreme weakness of the HI line, together with the lack of spatial resolution at low frequencies, makes it very difficult to fully characterize this component. If it represents a truly driving wind, the data from L1551 and HH7-11 suggest velocities of about 200 $\mathrm{km\,s^{-1}}$ and YSO mass loss rates of several 10^{-6} $\mathrm{M_\odot\ yr^{-1}}$

(Giovanardi et al. 1992)

For the case of an ionized driving wind, a component of potential interest is that detected at cm wavelengths (see recent review by Rodríguez 1997). The spectral index of this emission is usually consistent with models of free-free emission from an ionized wind, and in cases where the emission has been spatially resolved, it is elongated along the outflow direction (e.g., Anglada 1995). The momentum content of this component, however, is typically one or two orders of magnitude lower than the momentum in molecular outflows (Snell & Bally 1986), so it cannot by itself drive molecular flows. This component probably represents gas shock ionized by the outflow driving wind, so it constitutes a consequence, not a cause, of the bipolar outflow.

A final candidate for the outflow driving wind is the gas seen at optical and IR wavelengths in the form of Herbig-Haro objects and jets (see chapter by Reipurth & Raga in this volume for a more comprehensive discussion). As in the cm-wave emitting component, the momentum in the optically visible component is much too small to power molecular outflows (Mundt, Brugel, & Buhrke 1987), although this component is probably accompanied by a large amount of neutral gas, as jets seem lightly (few percent) ionized (Raga et al. 1990, Hartigan et al. 1994). This neutral component (invisible jet) has enough energy and momentum to drive in principle a weak molecular outflow (Hartigan et al. 1994), so it cannot be ruled as the outflow driving wind. Unfortunately, the lack of direct observability of this neutral component, together with the short radiative time of the HH objects and jets, makes it only possible to study the location of the most recent interaction, and the optical emission does not provide a complete history of the wind. The recent identification of large scale (super) jets (Bally & Devine 1997; Reipurth et al. 1997; see also the chapter by Reipurth & Raga in this volume) may help to circumvent this problem.

In summary, we do not have a conclusive direct observation of the primary agent which drives molecular outflows. Jets with large amounts of energy and momentum are present, and they seem to be largely neutral, but we cannot rule out that there exists a wide angle atomic component coexisting with the neutral jet and contributing to the outflow acceleration. Determining the nature of this agent, its collimation and velocity, remains the most critical problem in outflow research.

7.2. MODELS

It is not possible to make justice in the little space of this section to the enormous theoretical effort dedicated to modeling the outflow phenomenon and its many features. Here we will limit ourselves to reviewing a small sample of this work, distinguishing two types of models: those which attempt to explain the molecular gas acceleration starting with a given driving agent (jet, wide angle wind), and those which attempt to explain the outflow launching by the central star/disk system. Models from the first type are necessarily incomplete, as their goal is to *reproduce* outflow observations, leaving unanswered the question of how the primary wind is produced in first place. However, they permit an easy comparison with observations and therefore allow one to infer properties of the driving wind (collimation, velocity, etc). Models from the second type attempt to *produce* the outflow from first principles, and their goal is to offer the complete picture of the outflow phenomenon, from the launching of the wind to the acceleration the ambient cloud. The complexity of the whole process makes them harder to compare with observational data.

7.2.1. *Models of Molecular Gas Acceleration*

We first discuss models that start with some form of wind and study its propagation through the cloud, giving rise to a molecular outflow. For further details, we refer the reader to the excellent and up-to-date comparison between models and observations by Cabrit, Raga, & Gueth (1997). Models can be divided according to the agent collimation in jets and wide angle winds, a dichotomy that reflects the distinction between classical and highly collimated outflows discussed in the previous sections. Not surprisingly, each type of model reproduces well one of the two types of outflows, but has more difficulty explaining the other. Achieving a model which can reproduce both outflow types and can explain the transition between them remains an unfulfilled challenge.

Wide angle winds. Among wide angle models, the one by Shu et al. (1991) is probably the best studied. In this model, a YSO is embedded in a dense core with a density distribution that radially decreases as r^{-2} (Shu 1977) and has a flattening term $Q(\theta)$, where θ is the polar coordinate. A wind from the YSO emerges with an angular distribution which depends on the same polar angle θ through a function $P(\theta)$. As the wind propagates, it sweeps ambient medium forming a thin shell which constitutes the molecular outflow. Momentum conservation in every direction θ gives rise to a velocity law that depends angularly as $\sqrt{P(\theta)/Q(\theta)}$, which therefore defines the shape of the shell.

In their original paper, Shu et al. (1991) favored smooth forms for both $P(\theta)$ and $Q(\theta)$ at all angles, in order to reproduce the shapes of known outflows. Masson & Chernin (1992), however, pointed out that such choices of P and Q give rise to distributions of mass with velocity (and therefore to spectral profiles) that have too much gas at high velocities, in contradiction with observations. In a more recent elaboration of the wide-angle wind model, Li & Shu (1996) favor density distributions with little gas along the polar axis ("toroids") and winds with a stronger axial momentum component, avoiding the problem of the mass distribution while still producing reasonably-looking shells. Although the Li & Shu (1996) model seems to reproduce the main characteristics of classical outflows, it is not clear whether it can do the same with highly collimated molecular flows like HH211 (it does reproduce optical images from jets, see Shang et al. 1998). Also, if outflows evolve self similarly (Shu et al. 1991), it seems difficult to explain both the classical and highly collimated outflows. Still, it is possible that further refinements of this model (including time variability, for example) can reproduce these and other aspects, like EHV bullets.

Jet models. Jet-driven outflow models have attracted increasing interest after the discovery of the highly collimated outflows in the early 90's. As one could expect, this family of models reproduces best the highly collimated flows, but has more difficulty explaining classical outflows. Masson & Chernin (1993) have nicely discussed the basic physics involved in the driving of a molecular outflow by a jet. They argue that for molecular cloud densities ($n \sim 10^3 - 10^4$ cm^{-3}) and typical jet velocities (~ 300 km s^{-1}), the jet-cloud interaction is highly dissipative and a narrow bow shock forms at the jet end; the swept up material is accelerated mostly forward. Parameterizing the complicated bow shock physics in simple terms and adjusting the parameters from HH jet observations, Masson & Chernin (1993) construct a jet driven outflow model which they compare with observations. They succeed reproducing several observed features like the forward momentum, "Hubble-law" behavior, and distribution of mass with velocity, but their model produces jets that are too long and thin if they are allowed to evolve for several 10^5 yr (expected outflow lifetime, Parker et al. 1991). Masson & Chernin argue that this problem can be circumvented if the jet is allowed to wonder in angle, so it accelerates different pieces of gas with time, increasing the lobes width but limiting their length.

Another analytical model to reproduce a jet driven outflow is due to Raga & Cabrit (1993), who consider the situation of an internal jet working surface caused by time dependence in the flow velocity field. In this model, a bow shock compresses and sweeps ambient material, which later re-expands into the cavity left behind, forming a turbulent wake identified with the molecular flow. With this model, and assuming the size of the bow shock increases with distance (due to the cloud density decreasing away from the YSO), Raga & Cabrit reasonably reproduce observed shapes of outflows. Their distribution of mass decreases with velocity, as observed in molecular outflows, although the decrease seems too rapid, producing triangular spectra.

In addition to the above analytical models (and others due to Stahler 1993, Wilkin 1996, Zhang & Zheng 1996), numerical simulations of the propagation of a jet through a cloud have been presented by a number of authors (e.g. Chernin et al. 1994, Stone & Norman 1994, Raga et al. 1995, Frank & Mellema 1996, Smith et al. 1997, Suttner et al. 1997). Unfortunately, it is difficult to follow the evolution of a high velocity jet moving at several hundred $\mathrm{km\,s^{-1}}$ over the time scales typical of outflows (several 10^5 yr), so only the early stages of the outflow production can be investigated in this way. Hopefully, longer calculations will be possible in the next future, opening the possibility of comparing numerical simulations with CO observations of mature outflows.

7.2.2. *Wind Launching Models*

Although a variety of theories was proposed soon after the discovery of bipolar outflows (e.g., Barral & Cantó 1981, Königl 1982, Torbett 1984), only the family of magnetohydrodynamic (MHD) models seems to have survived the test of time. As pointed out by De Campli (1981), thermal expansion and line radiation pressure are not efficient enough driving the winds observed in some TTauri stars, which are most likely weaker than those at the origin of bipolar flows. MHD models seem capable to do the job and to meet the energy and momentum requirements by converting a fraction of the gravitational energy released by mass accretion into outflow motion. This is achieved by the coupling of gas rotation with the magnetic field, in a mechanism analogous to the behavior of a bead on a rotation, rigid wire (Henriksen & Rayburn 1971). In this situation, if the magnetic field is coupled to the rotating matter (through flux freezing) and if it makes a sufficiently large angle with the totation axis ($> 30°$), corrotation accelerates and ejects the material along the field lines. Achieving a geometry where the magnetic field makes such an angle with the rotation vector is the crucial point in launching the outflow.

The above situation can be obtained in at least two configurations. In one, the outflow arises from a disk which is threaded by an inclined (concave) magnetic field (Blandford & Payne 1982). In the other, the outflow arises from the surface of the star, taking advantage of the natural curvature of the stellar surface near the equator (Belcher & MacGregor 1976).

The original disk outflow models (Pudritz & Norman 1983, Pudritz 1985, Uchida & Shibata 1985) required very massive disks (several $M_\odot$), which are not supported by observations. More modern versions of this model (Königl 1989, 1995, Lovelace et al. 1991, Ferreira & Pelletier 1993) use much more reasonable parameters. One nice feature of a wind model is that the wind can carry away part of the angular momentum, allowing disk accretion without the need for an anomalous viscosity (Pudritz 1985). The main criticism to this model (Shu et al. 1987) is the difficulty of producing a strong bend in the magnetic field, necessary to launch the wind, against the natural trend of the magnetic lines to straighten up.

The alternative situation was proposed by Shu et al. (1988) (see also Hartmann & MacGregor 1982), with the outflow being launched from the stellar surface, near the equator. This so-called X-wind mechanism is explained with detail in the chapter by Shu in this book. In this model, a magnetic field, emerging almost perpendicular to the star surface, makes the adequate angle to centrifugally drive a wind. For this to happen, however, the star should be rotating near break up velocity, which is much faster than observed in TTauri stars (Bouvier et al. 1986, Hartmann et al. 1986). A more recent elaboration of this model (Shu et al. 1994a, b; Najita & Shu 1994) avoids this problem by having the strong stellar magnetic field truncate the disk at some distance from the stellar surface. This point, located where the disk material corrotates with a slower rotating star, provides a strong lever arm for launching energetic winds; both the bipolar outflow and an infall funnel flow emerge from this X-radius.

Acknowledgements. It is a pleasure to acknowledge Drs. André, Bontemps, Cabrit, Cernicharo, Codella, Colomer, Dutrey, Fuente, Gueth, Guilloteau, Martín-Pintado, Myers, Pérez Gutiérrez, Planesas, Reipurth, Richer, Shu, and Walmsley for interesting discussions and in many cases for fruitful collaborative work on outflows over the past several years. Funding support from Spanish DGES grant PB96-104 is also gratefully acknowledged.

References

Adams, F.C., Lada, C.J., Shu, F.H. 1987. ApJ 312, 788
Allamandola, L.J., Sandford, S.A., Tielens, A.G.G.M., Herbst, T. 1992, ApJ 399, 134
André, P. 1997 in *IAU Symposium No. 182*, eds. B. Reipurth and C. Bertout (Kluwer Academic Publishers), p. 483
André, P., Martín-Pintado, J., Despois, D., Montmerle, T. 1990, A&A 236, 180
André, P., Ward-Thompson, D., Barsony. M. 1993, ApJ 406, 122
Anglada, G. 1995, Rev. Mex. Astron. Astrofís. Ser. de Conf. 1, 67
Anglada, G., Estalella, R., Rodríguez, L.F., Torrelles, J.M, López, R., Cantó, J. 1991, ApJ 376, 615
Avery, L.W., Hayashi, S.S., White, G.J. 1990, ApJ 357, 524
Avery, L.W., Chiao, M. 1996, ApJ 463, 642
Bachiller, R. 1996, ARAA 34, 111
Bachiller, R., Cernicharo, J. 1990 A&A 239, 276
Bachiller, R., Gómez-González, J. 1992 A&A Review 3, 257
Bachiller, R., Cernicharo, J., Martín-Pintado, J., Tafalla, M., Lazareff, B. 1990 A&A 231, 174
Bachiller, R., Codella, C., Colomer, F., Liechti, S., Walmsley, C.M. 1998, A&A 335, 266
Bachiller, R., Fuente, A., Tafalla, M. 1995a, ApJ 445, L51
Bachiller, R., Guilloteau, S., Dutrey, A., Planesas, P., Martín-Pintado, J. 1995, A&A 299, 857
Bachiller, R., Guilloteau, S., Gueth, F., Tafalla, M., Dutrey, A., Codella, C., Castets, A.

1998, A&A, in press
Bachiller, R., Liechti, S., Walmsley, C.M., Colomer, F. 1995, A&A 295, L51
Bachiller, R., Martín-Pintado, J., Fuente, A. 1991a, A&A 243, L21
Bachiller, R., Martín-Pintado, J., Fuente, A. 1993, ApJ 417, L45
Bachiller, R., Martín-Pintado, J., Planesas, P. 1991b, A&A 251, 639
Bachiller, R., Pérez Gutiérrez, M. 1997, ApJ 487, L93
Bachiller, R., Tafalla, M., Cernicharo, J. 1994, ApJ 425, L93
Bally, J. 1982, ApJ 262, 558
Bally, J. 1986, Can. J. Phys. 64, 383
Bally, J., Lada C.J. 1983. ApJ 265, 824
Bally, J., Lane A.P. 1991, in *The Physics of Star Formation and Early Stellar Evolution*, ed. C.J. Lada and N.D. Kylafis (Kluwer, Dordrecht), pag. 471
Bally, J., Stark, A.A. 1983, ApJ 266, L61
Bally, J., Devine, D. 1997, in IAU Symp. 182 *Herbig-Haro Flows and the Birth of Low Mass Stars* (Eds. B. Reipurth & C. Bertout). Kluwer, Dordrecht, pag. 29
Barral, P., Cantó, J. 1981 Rev. Mex. Astron. Astrofís. 5, 101
Belcher, J. W., MacGregor, K.B. 1976, ApJ 210, 498
Bence, S.J, Padman, R., Isaak, K.G., Wiedner, M.C., Wright, G.S. 1998, MNRAS 299, 965
Bergin, E.A., Neufeld, D. A., Melnick, G.J. 1998, ApJ 499, 777
Bernstein, M.P., Sandford, S.A., Allamandola, L.J., Chang, S., Scharberg, M.A. 1995, ApJ 454, 327
Blake, G.A. 1996, in IAU Symp. 178, Molecules in Astrophysics: Probes and Processes (ed. E.F. van Dishoeck). Kluwer, Dordrecht, pag. 31
Blake, G.A., Sutton, E.C., Masson, C.R., Phillips, T.G. 1987, ApJ 315, 621
Blake, G.A., van Dishoeck, E.F., Jansen, D.J., Groesbeck, T.D., Mundy, L.G. 1994, ApJ 428, 680
Blake, G.A., Sandell, G., van Dishoeck E.F., Groesbeck, T.D., Mundy, L.G., Aspin, C. 1995, ApJ 441, 689
Blandford, R.D., Payne, D.G. 1982, MNRAS 199, 883
Bontemps, S., André, P., Terebey, S., Cabrit, S. 1996. A&A 297, 98
Bouvier, J., Bertout, C., Benz, W., Mayor, M. 1986, A&A 165, 110
Bourke, T.L, Garay, G., Lehtinen, K.K., Koehnenkamp, I., Launhardt, R., Nyman, L.A., May, J., Robinson, G., Hyland, A.R. 1997, ApJ 476, 781
Cabrit, S., Bertout, C. 1986. ApJ 307, 313
Cabrit, S., Bertout, C. 1990. ApJ 348, 530
Cabrit, S., Bertout, C. 1992. A&A 261, 274
Cabrit, S., Goldsmith, P.F., Snell, R.L. 1988. ApJ 334, 196
Cabrit, S., Raga, A.C., Gueth, F. 1997, in IAU Symp. 182 *Herbig-Haro Flows and the Birth of Low Mass Stars* (Eds. B. Reipurth & C. Bertout). Kluwer, Dordrecht, pag. 163
Cabrit, S., Couturier, Andre, P., Boulade, O., Cesarsky, C. J. and Lagage, P. O., Sauvage, M., Bontemps, S., Nordh, L. and Olofsson, G., Boulanger, F., Sibille, F., Siebenmorgen, R. 1998. In *ASP Conf. Ser. 132: Star Formation with the Infrared Space Observatory*, eds. Yun, J. and Liseau, R. (ASP), pag. 326
Cantó, J., Rodriguez, L.F., Barral, J.F., Carral, P. 1981, Apj 244, 102
Caselli, P., Hartquist, T.W., Havnes, O. 1997, A&A 322, 296
Ceccarelli, C., Haas, M. R., Hollenbach, D. J., Rudolph, A. L. 1997. ApJ 476, 771
Cernicharo, J., Reipurth, B.1996. ApJ 460, L57
Charnley, S.B. 1997, ApJ 481, 396
Chernin, L.M., Masson, C.R., Fuller, G. 1994, ApJ 436, 741
Choi, M., Evans, N.J. II, Jaffe, D.T. 1993, ApJ 417, 624
Clark, F.O., Laurejis, R.J. 1986, A&A 154, L26
Codella, C., Bachiller, R., Reipurth, B. 1999, A&A, in press
Cohen, M., Bieging, J.H., Schwartz, P.R. 1982, ApJ 253, 707

Cohen, M., Hollenbach, D. J., Haas, M. R. and Erickson, E. F. 1988, ApJ 329, 863
Cudworth, K.M., Herbig, G.H. 1979, Astron. J. 84, 548
Davis, J.J., Eisloeffel, J. 1995, A&A 300, 851
De Campli, W.M. 1981, ApJ 244, 124
Draine, B.T., Roberge, W.G., Dalgarno, A. 1983, ApJ 264, 485
Dutrey, A., Guilloteau, S., Bachiller, R., 1997 A&A 325, 758
Edwards, S., Snell, R.L. 1982, ApJ 261, 151
Edwards, S., Snell, R.L. 1983, ApJ 270, 605
Edwards, S., Snell, R.L. 1984, ApJ 281, 237
Edwards, S., Strom, S.E., Snell, R.L., Jarrett, T.H., Beichman, C.A., Strom, K.M. 1986, ApJ 307, L65
Frank, A., Mellema, G. 1996, ApJ 472, 684
Ferreira, J., Pelletier, G. 1993, A&A 276, 625
Fukui, Y., Iwata, T., Mizuno, A., Bally, J., Lane, A.P. 1993, in *Protostars and Planets III*, ed. EH Levy, JI Lunine. Tucson: Univ. Ariz. Press
Garay, G., Köhnenkamp, I., Bourke, T.L., Rodríguez, L.F., Lehtinen, K.K. 1998, ApJ, in press
Garden, R.P., Hayashi, M., Gatley, I., Hasegawa, T., Kaifu, N. 1991, ApJ 374, 540
Gibb, A.G., Davis, C.J., 1998, MNRAS 298, 644
Giovanardi, C., Lizano, S., Natta, A., Evans, N.J. II, Heiles, C. 1992, ApJ 397, 214
Graham, J.A., Heyer, M.H. 1990, PASP 102, 972
Gueth, F., Guilloteau, S. 1999, A&A, in press
Gueth, F., Guilloteau, S., Bachiller, R. 1996, A&A 307, 891
Gueth, F., Guilloteau, S., Dutrey, A., Bachiller, R. 1997, A&A 323, 943
Guilloteau, S., Bachiller, R., Lucas, R., Fuente, A. 1992, A&A 265, L49
Haro, G. 1952, ApJ 115, 572
Hartigan, P., Morse, J. and Raymond, J. 1994, ApJ 436, 125
Hartmann, L., Hewett, R., Stahler, S., Mathieu, R.D. 1986, ApJ 309, 275
Hartmann, L., MacGregor, K.B. 1982, ApJ 259, 180
Henriksen, R.N., Rayburn, D.R. 1971, MNRAS 152, 152
Herbig, G. 1951, ApJ 113, 697
Herbig, G. 1962, Avd. A&A 1, 47
Hodapp, K.W. 1994, ApJSS 94, 615
Hodapp, K.W., Ladd, E.F. 1995, ApJ 453, 715
Hollenbach, D. 1985, Icarus 61, 36
Kaufman, M. J., Neufeld, D.A. 1996, ApJ 456, 611
Kitamura, Y., Kawabe, R., Yamashita, T., Hayashi, M. 1990, ApJ 363, 180
Kitamura, Y., Kawabe, R., Ishiguro, M. 1992, PASJ 44, 407
Königl, A. 1982, ApJ 261, 115
Königl, A. 1989, ApJ 342, 208
Königl, A. 1995, Rev. Mex. Astron. Astrofís. (Ser. de Conf.) 1, 275
Koo, B.-C. 1989, ApJ 337, 318
Koo, B.-C. 1990, ApJ 361, 145
Kuhi, L.V. 1964 ApJ 140, 1409
Kuiper, T.B.H., Zuckerman, B., Rodríguez-Kuiper, E.N. 1981, ApJ 251, 88
Kwan, J., Scoville, N. 1976, ApJ 210, L39
Lada, C.J. 1985, ARAA 23, 267
Lada, C.J. 1991, in *The Physics of Star Formation and Early Evolution*, eds. CJ Lada, ND Kylafis. Kluwer: Dordrecht
Lada, C.J., Fich, M. 1996, ApJ 459, 638
Langer, W.D., Castets, A., Lefloch, B. 1996, ApJ 471, 111
Levreault, R.M. 1988, ApJSS 67, 283
Li, Z.-Y., Shu, F.H. 1996, ApJ 468, 261
Lizano, S., Heiles, C., Rodriguez, L.F., Koo, B., Shu, F.H., Hasegawa, T., Hayashi, S., Mirabel, I.F. 1988, ApJ 328, 763

Lovelace, R.V.E., Berk, H.L., Contopoulos, J. ApJ 376, 696
Margulis, M., Lada, C.J. 1985, ApJ 299, 925
Margulis, M., Snell, R.L. 1989, ApJ, 343, 779
Martín-Pintado, J., Bachiller, R., Fuente, A. 1992, A&A 254, 315
Masson, C.R., Chernin, L.M. 1992, ApJ 387, L47
Masson, C.R., Chernin, L.M. 1993, ApJ 414, 230
Masson, C.R., Mundy, L.G., Keene, J. 1990, ApJ 357, L25
Mathieu, R.D. 1994, ARAA 32, 465
Mathieu, R.D., Benson, P.J., Fuller, G.A., Myers, P.C., Schild, R.E. 1988, ApJ 330, 385
McCaughrean, M.J., Rayner, J.T., Zinnecker, H. 1994, ApJ 436, L189
Meyers-Rice, B.A., Lada, C.J. 1991, ApJ 368, 445
McMullin, J.P., Mundy, L.G., Blake, G.A. 1994, ApJ 437, 305
Mikami, H., Umemoto, T., Yamamoto, S., Saito, S. 1992, ApJ 392, L87
Moriarty-Schieven, G.H., Snell, R.L. 1988, ApJ 332, 364
Moriarty-Schieven, G.H., Snell, R.L. 1989, ApJ 338, 952
Moriarty-Schieven, G.H., Snell, R.L., Hughes, V.A. 1989, ApJ 347, 358
Mundt, R., Brugel, E.W., Bührke, T. 1987, ApJ 319, 275
Mundt, R, Fried, J.W. 1983, ApJ 274, L83
Myers, P.C., Heyer, M., Snell, R.L., Goldsmith, P.F. 1988, ApJ 324, 907
Myers, P.C., Ladd, E.F. 1993, ApJ 413, L47
Nagar, N.M., Vogel, S.N., Stone, J.M., Ostriker, E.C. 1997, ApJ 482, 195
Najita, J.R., Shu, F.H. 1994, ApJ 429, 808
Neufeld, D.A., Kaufman, M.J. 1993, ApJ 418, 263
Nisini, B., Giannini, T., Molinari, S., Saraceno, P., Caux, E., Ceccarelli, C., Liseau, R., Lorenzetti, D., Tommasi, E., White, G. J. 1998, in *ASP Conf. Ser. 132: Star Formation with the Infrared Space Observatory*, eds. Yun, J. and Liseau, R. (ASP), p. 256
Osterbrock, D.E. 1958, PASP 70, 399
Padman, R., Bence, S., Richer, J. 1997, in *IAU Symposium No. 182*, eds. B. Reipurth and C. Bertout (Kluwer Academic Publishers), p. 123
Parker, N.D., Padman, R., Scott, P.F. 1991, MNRAS 252, 442
Pineau des Forêts, G., Flower, D.R., Chièze, J.P. 1997, in IAU Symp. 182 *Herbig-Haro Flows and the Birth of Low Mass Stars* (Eds. B. Reipurth & C. Bertout). Kluwer, Dordrecht, pag. 199
Plambeck, R.L., Snell, R.L., Loren, R.B. 1983. ApJ 266, 321
Pudritz, R.E. 1985, ApJ 293, 216
Pudritz, R.E., Norman, C.A. 1983, ApJ 274, 677
Raga, A.C., Cabrit, S. 1993, A&A 278, 267
Raga, A.C., Binette, L., Cantó, J. 1990, ApJ 360, 612
Raga, A.C., Taylor, S.D., Cabrit, S., Biro, S. 1995, A&A 296, 833
Reipurth, B., Bally, J., Devine, D. 1997, AJ 114, 2708
Richer, J.S., Hills, R.E., Padman, R. 1992, MNRAS, 254, 525
Richer, J., Shepherd, D., Cabrit, S., Bachiller, R., Churchwell, E. 1999, in *Protostars & Planets IV*, in press
Rodríguez, L.F. 1995, Rev. Mex. Astron. Astrofís. (Ser. de Conf.) 1, 1
Rodríguez, L.F. 1997, in IAU Symp. 182 *Herbig-Haro Flows and the Birth of Low Mass Stars* (Eds. B. Reipurth & C. Bertout). Kluwer, Dordrecht, pag. 83
Rodríguez, L.F., Ho, P.T.P., Moran, J.M. 1980, ApJ 240, L149
Rodríguez, L.F., Lizano, S., Cantó, J., Escalante, V., Mirabel, I.F. 1990, ApJ 365, 261
Saraceno, P., André, P., Ceccarelli, C., Griffin, M., Molinari, S. 1996, A&A 309, 827
Saraceno, P., Nisini, B., Benedettini, M., Ceccarelli, C., Di Giorgio, A. M., Giannini, T., Molinari, S., Spinogl, L., Clegg, P. E., Correia, J., Griffin, M. J., Leeks, S. J., White, G. J., Caux, E., Lorenzetti, D., Tommasi, E., Liseau, R., Smith, H. A. 1998, in *ASP Conf. Ser. 132: Star Formation with the Infrared Space Observatory*, eds. Yun, J. and Liseau, R. (ASP), p. 233

Schilke, P., Walmsley, C.M, Pineau des Forêts, G., Flower, D.R. 1997, A&A 321, 293
Schutte, W.A., Gerakines, P.A., Geballe, T.R., van Dishoeck, E.F., Greenberg, J.M. 1996, A&A 309, 633
Schwartz, R.D. 1975, ApJ 195, 631
Shang, H., Shu, F.H., Glassgold, A.E. 1998, ApJ 493, L91
Shu, F.H. 1977, ApJ 214, 488
Shu, F.H., Adams, F.C., Lizano, S. 1987, ARAA 25, 23
Shu, F.H., Lizano, S., Ruden, S.P., Najita, J. 1988, ApJ 328, L19
Shu, F.H., Najita, J., Ostriker, E., Wilkin, F., Ruden, S.P., Lizano, S. 1994a, ApJ 429, 781
Shu, F.H., Najita, Ruden, S.P., Lizano, S. 1994b, ApJ 429, 797
Shu, F.H., Najita, J.R., Shang, H., Li, Z.-Y. 1999, in *Protostars & Planets IV*, in press
Shu, F.H., Ruden, S.P., Lada, C.J., Lizano, S. 1991, ApJ 370, L31
Shull, J.M., Beckwith, S. 1982, ARAA 20, 163
Smith, M.D. 1994, MNRAS 266, 238
Smith, M.D., Suttner, G., Yorke, H.W. 1997, A&A 323, 223
Snell, R.L.: 1987, in *IAU Symposium No. 115: Star Forming Regions*, eds. M. Peimbert and J. Jugaku (Reidel, Dordrecht), p. 213
Snell, R.L., Bally, J. 1986, ApJ 303, 683
Snell, R.L., Loren, R.B., Plambeck, R.L. 1980, ApJ 239, L17
Snell, R.L., Scoville, N.Z., Sanders, D.B., Erickson, N.R. 1984, ApJ 284, 176
Stahler, S.W. 1993, in *Astrophysical Jets*, ed. M Livio, C O'Dea, D. Burgarella. Cambridge: Cambridge University Press
Staude, H.J., Elsässer, H. 1993, A&A Rev. 5, 165
Stone, J.M., Norman, M.L. 1994, ApJ 420, 237
Suttner, G., Smith, M.D., Yorke, H.W., Zinnecker, H. 1997, A&A 318, 595
Tafalla, M., 1993, Ph. D., Univ. of California, Berkeley
Tafalla, M., Bachiller, R. 1995, ApJ 443, L37
Tafalla, M., Bachiller, R., Wright, M.C.H. 1994, ApJ 432, L127
Tafalla, M., Bachiller, R., Wright, M.C.H., Welch, W.J. 1997, ApJ 474, 329
Torbett, M.V. 1984, 278, 318
Torrelles, J.M., Rodríguez, L.F., Cantó, J., Carral, P., Marcaide, J., Moran, J.M., Ho, P.T.P., 1983, ApJ 274, 214
Uchida, Y., Shibata, K. 1985, PASJ 37, 515
Umemoto, T., Iwata, T., Fukui, Y., Mikami, H., Yamamoto, S., Kamaya, O., Hirano, N. 1992, ApJ 392, L83
van Dishoeck, E.F., Blake, G.A. 1998, ARAA, in press
van Dishoeck, E.F., Blake, G.A., Jansen, D.J., Groesbeck, T.D. 1995, ApJ 447, 760
Velusamy, T., Langer, W.D. 1998, Nature 392, 685
Wilkin, F.P. 1996, ApJ 459, 31
Wolf, G.A., Lada, C.J., Bally, J. 1990, AJ 100, 1892
Wootten, A., Loren, R.B., Sandqvist, A., Friberg, P., Hjalmarson, A. 1984, ApJ 279, 633
Wu, Y., Huang, M., He, J. 1996, A&ASS 115, 283
Zhang, Q., Ho, P.T.P., Wright, M.C.H., Wilner, D.J. 1995, ApJ 451, L71
Zhang, Q., Zheng, X. 1997, ApJ 474, 719
Zinnecker, H., McCaughrean, M.J., Rayner, J.T. 1998, Nature 394, 862